

Review

A Comprehensive Review on Transient Recovery Voltage in Power Systems: Models, Standardizations and Analysis

Eleonora Fripp Lazzari ^{1,*}, Adriano Peres de Morais ¹, Maicon Ramos ², Renato Ferraz ³, Tiago Marchesan ¹, Vitor Cristiano Bender ¹, Rodinei Carraro ⁴, Herber Fontoura ⁴, Cristian Correa ⁴ and Mariana Resener ^{5,*}

¹ Graduate Program in Electrical Engineering, Federal University of Santa Maria, Santa Maria 97105-900, Brazil; adriano@ctism.ufsm.br (A.P.d.M.); tiago@ufsm.br (T.M.); vitor.bender@ufsm.br (V.C.B.)

² Siemens Canada Limited, Smart Infrastructure, Richmond, BC V6V 2K9, Canada; maicon.ramos@siemens.com

³ Interdisciplinary Department, Federal University of Rio Grande do Sul, Tramandai 95590-000, Brazil; renato.ferraz@ufrgs.br

⁴ CPFL Transmission, Porto Alegre 90230-181, Brazil; rodinei.carraro@cpfl.com.br (R.C.); herber.fontoura@cpfl.com.br (H.F.); cristian.correa@cpfl.com.br (C.C.)

⁵ School of Sustainable Energy Engineering, Faculty of Applied Sciences, Simon Fraser University-Surrey Campus, Surrey, BC V3T 0N1, Canada

* Correspondence: eleonora.lazzari@acad.ufsm.br (E.F.L.); mresener@sfu.ca (M.R.)

Abstract: Electrical power systems are exposed to transient disturbances that change the voltage and current signals of the network, which can interrupt power and damage equipment. In high-frequency phenomena, it is essential to study the transient recovery voltage (TRV) to ensure the electrical insulation limits of circuit breakers are not violated, thus leading to a safe and reliable operation. Adequate models are crucial to achieving satisfactory results in the studies, according to the range of frequency of the transient being evaluated. This paper presents a comprehensive literature review of methods and models for studying electromagnetic transients, focusing on TRV requests imposed on circuit breakers, in addition to fault-clearing simulations on real system modeling. The analyses are fundamental both for the evaluation of the amplitude of the voltage signal and for its rate of rise. We also compare the reviewed models and techniques to provide a handy resource for researchers.

Keywords: power systems; very fast transients; transient recovery voltage; reliability



Citation: Lazzari, E.F.; Morais, A.P.d.; Ramos, M.; Ferraz, R.; Marchesan, T.; Bender, V.C.; Carraro, R.; Fontoura, H.; Correa, C.; Resener, M. A

Comprehensive Review on Transient Recovery Voltage in Power Systems: Models, Standardizations and Analysis. *Energies* **2023**, *16*, 6348. <https://doi.org/10.3390/en16176348>

Academic Editor: Tek Tjing Lie

Received: 14 July 2023

Revised: 24 August 2023

Accepted: 25 August 2023

Published: 1 September 2023



Copyright: © 2023 by the authors. Licensee MDPI, Basel, Switzerland. This article is an open access article distributed under the terms and conditions of the Creative Commons Attribution (CC BY) license (<https://creativecommons.org/licenses/by/4.0/>).

1. Introduction

The electricity sector is undergoing substantial transformations, driven by the integration of variable renewable sources [1], deep electrification and various other factors tied to the energy transition [2]. Navigating these challenges demands a comprehensive approach combining technological innovation and policy recommendations to establish resilient and flexible energy systems. Moreover, as the electricity system undergoes profound transformations, the importance of modeling and analyzing various phenomena becomes even more pronounced, serving as a tool to ensure the safety and reliability of operations.

To ensure the reliable and safe operation of electrical power systems, it is crucial to effectively monitor and protect the various equipment inserted into the system. Among the equipment in the transmission system, the power transformer is particularly significant as any damage to it can have severe consequences for the network. The protection system needs to identify the type of fault that occurred and which equipment was affected, enabling the isolation of the specific area where the equipment is located. In order to obtain accurate simulation results, it is essential to correctly model not only the equipment itself but also the system to which it is connected. Therefore, conducting a preliminary study on the modeling requirements for different equipment in the network becomes imperative. For example, when dealing with transformers, it is important to consider various factors, such as different core topologies, winding configurations and linear and non-linear characteristics dependent on frequency, in order to accurately model such equipment.

According to [3–8], the voltages experienced by power equipment terminals can be categorized as either steady-state or transient. Generally, these equipment components operate under steady-state voltages, which typically fall within a range of 10% around the nominal value. However, transient overvoltages can occur due to events such as short circuits, switching operations, lightning strikes and changes in the normal operating conditions of the system [9].

Transient periods are of great importance as they subject circuit components to significant stress caused by excessive currents or voltages [3]. According to [10], transient overvoltages are characterized by their short duration, potential oscillatory nature and typically strong damping. Practical investigations documented in several literature sources highlight that transient overvoltages pose a threat not only due to their magnitude but also because of their rate of rise [11–13]. Consequently, frequent overvoltages with smaller amplitudes but high rate of rise can be just as hazardous as overvoltages with larger amplitudes [14]. In this sense, it becomes essential to study the peculiarity of the phenomena for a complete understanding of the behavior of electrical circuits [3].

Modelling of elements in electric power systems must consider the frequency of the events being studied, and it is still a challenge for high frequencies. Several papers addressing modeling techniques for different equipment can be found in the literature. Given the challenges involved in modeling power systems, we selected and reviewed the most relevant papers published from 1928 to 2023 in international conferences and journals, in addition to standards. To the best of our knowledge, no review paper addresses models for the analysis of TRV requests. Therefore, we aim to provide a handy resource for researchers in the field by presenting a comprehensive survey delving into a wide array of methods and models, specifically concentrating on examining TRV requests imposed on circuit breakers.

Given the context described thus far, the main contributions of this paper can be summarized as follows:

- we present a comprehensive survey on methods and models for studying electromagnetic transients in power systems, focusing on TRV requests imposed on circuit breakers;
- we present a case study based on data from a real substation to demonstrate the impacts of choosing the correct parameters when studying TRV;
- the study uniquely explores the influence of capacitances within equipment models on both TRV and the rate of rise of recovery voltage (RRRV).

This paper is organized as follows: Section 2 provides fundamental definitions of transients based on their frequency range, shape and typical sources of origin. Section 3 explores general aspects of transient recovery voltage analysis, focusing on the key standardizations related to circuit breakers and their response to this phenomenon. Section 4 presents the simulation of transient recovery voltage (TRV) for a modeled power system, along with an analysis of different scenarios and a discussion of the obtained results. Finally, in Section 5, the main conclusions regarding the findings throughout the paper are summarized.

2. Definitions and Characteristics

Phenomena classified as fast-front or very fast-front transients have the capacity to cause damage to components in distribution and transmission systems, including cables, power transformers and circuit breakers [15]. The interaction between devices with high-frequency characteristics can result in abnormal and detrimental alterations to the involved system. Table 1, adapted from [16], provides an overview of the primary sources of transients and their respective frequency ranges.

Table 1. Origin of electrical transients and frequency ranges (adapted from [16]).

Origin	Frequency Range							
	0.1–1 kHz	0.1–3 kHz	50/60 Hz–3 kHz	50/60 Hz–20 kHz	50/60 Hz–100 kHz	10 kHz–1 MHz	10 kHz–3 MHz	100 kHz–50 MHz
Transformer Energization Ferroresonance *	x							
Load Rejection		x						
Fault Clearing			x					
Fault Initiation				x				
Line Energization				x				
Load Reclosing *				x				
TRV—Terminal Faults				x				
TRV—Short-Line Faults					x			
Multiple Re-strikes of Circuit Breaker						x		
Lighting Surges, Faults in Substations							x	
Disconnecter Switching								x
Faults in Gas Insulated Substation								x

* Considered DC.

Table 2, adapted from [16], presents the classification of the transients in four frequency ranges, with their respective shape designation and main applications.

Table 2. Classification of transients according to the frequency range (adapted from [16]).

Frequency Range	0.1 Hz–3 kHz	60 Hz–20 kHz	10 kHz–3 MHz	100 kHz–50 MHz
Shape Designation	Low Frequency Oscillations	Slow Front Surges	Fast Front Surges	Very Fast Front Surges
Representation	Temporary Overvoltages	Switching Overvoltages	Lightning Overvoltages	Re-strike Overvoltages

Overvoltages that stress the insulation of equipment in an electrical system can be characterized by their amplitude, shape and duration. In order to represent the actual effects of these overvoltages, standard waveforms were established by [17] and are illustrated in Figure 1.

2.1. Characteristics of Equipment and Components for TRV

To adequately represent the equipment involved in a transient, it is necessary to determine which range of frequencies are associated with the investigated phenomenon [16]. The mathematical models developed to describe the system’s equipment must be in accordance with the conditions imposed on its operation. Thus, in many cases, it is necessary to have three-phase modeling, considering interactions and couplings between phases and frequency variations. However, several equivalent single-phase models are developed to simplify studies in nominal frequencies, such as in steady-state. In general, steady-state analysis involve simpler models, while the complexity increases when transient studies are carried out.

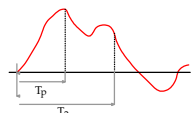
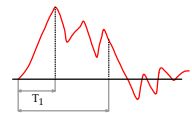
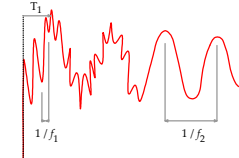
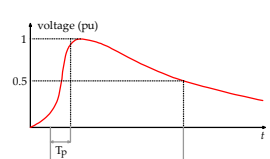
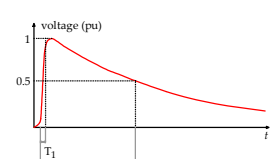
Class	Transient		
	slow-front	fast-front	very-fast-front
voltage or over-voltage shapes	 <p>$20 \mu s < T_p \leq 5000 \mu s$ $T_2 \leq 20 \text{ ms}$</p>	 <p>$0.1 \mu s < T_1 \leq 20 \mu s$ $T_2 \leq 300 \mu s$</p>	 <p>$3 \text{ ns} < T_1 \leq 100 \text{ ns}$ $0.3 \text{ MHz} < f_1 < 100 \text{ MHz}$ $30 \text{ kHz} < f_2 < 300 \text{ kHz}$</p>
standard voltage shapes	 <p>$T_p = 250 \mu s$ (front time) $T_2 = 25000 \mu s$ (tail time)</p>	 <p>$T_1 = 1.2 \mu s$ (front time) $T_2 = 50 \mu s$ (tail time)</p>	
standard withstand test	switching impulse test	lightning impulse test	

Figure 1. Classes and shapes of overvoltages: standard voltage shapes and standard withstand tests (adapted from [17]).

In transient analysis, one critical aspect is that a physical component can have different representation models. The model representation is directly linked to the specific transient phenomenon being investigated [18]. For instance, one can represent a transformer by an inductance, a network of capacitances or a combination of both. Further, according to the nature of the studied study, the non-linearity of the magnetic core may have relevance. The expected results of the study in question, as well as the prior knowledge of the applied phenomenon, help to determine the best model for the physical component of the system [18]. Table 3, adapted from [16], presents the substation equipment and its modeling relevance for different frequency ranges.

Table 3. Classification of frequency ranges.

Substation	Group I	Group II	Group III	Group IV
Equipment	0.1 Hz–3 kHz	60 Hz–20 kHz	10 kHz–3 MHz	100 kHz–50 MHz
Transformer Capacitance	Negligible	Important	Important $C > 0.5 \text{ nF}$	Very Important
Transformer Inductance	Negligible	Negligible	Negligible	Important
Transformer Saturation	Important	Negligible	Negligible	Negligible
Surge Arresters	Negligible	Negligible	Very Important	Very Important
Transmission Line Capacitance	Negligible	Negligible	Important	Very Important
Circuit Breaker	Negligible	Negligible	Very Important	Very Important
Potential and Current Transformer	Negligible	Negligible	Important	Very Important

The turn-to-turn capacitance is normally neglected at low frequencies; however, for high-frequency events, its representation becomes significant. When the system is subjected to a pulse test, the capacitance determines the voltage distribution between the transformer's internal windings. In addition, the capacitance between the turns and the inductance of the winding has a resonant frequency that can be excited. Therefore, transformer failures can be caused by high-frequency overvoltages due to internal resonances [19,20].

The internal winding resonances, generally in the 5 to 200 kHz range, are initiated by fast transients and may not cause immediate damage. However, partial discharges may occur, accelerating the aging of the transformer winding [21]. A detailed high-frequency transformer model is needed to determine the voltage levels across transformer insulation during the specific external transients. Although high-frequency general models are accurate and precise, they are often too large to incorporate into an overall power system model [22].

The study of overvoltages in a transmission system is crucial for investigating transients as it facilitates equipment specification and the coordination of line and substation isolation. Different types of overvoltages are generated in the system, categorized based on the degree of damping and their respective time constants. These types include temporary, switching and lightning-induced overvoltages [23]. In [24], an artificial neural network (ANN)-based approach to determine overvoltages in power systems is observed. The authors of [25] also developed an ANN algorithm for locating faults based on Stockwell transform on TRV.

The temporary overvoltage is an overvoltage at a given point in the system, being phase-to-ground or between phases, oscillating and with relatively long duration, with a total time more than 10 ms [17]. Phenomena that characterize temporary overvoltage consist of switching operation of circuit breakers and fault-clearing events [26].

Switching overvoltage is also a phase-to-ground or phase-to-phase overvoltage at a given point in the system and occurs due to the operation of a switchgear or a fault, generally classified as strongly damped and of short duration. Still, it normally has a unidirectional or oscillating front, highly damped voltage and usually caused by switching or faults [27].

It is worth mentioning that the expression "short duration" used in the following definitions consists of characterizing the overvoltage in terms of the wavefront time and the time until the half value. Overvoltages with a front time between 100 and 500 μs , frequencies between 10 kHz and 2 kHz and with a time up to the middle value of the order of 2500 μs are generally considered switching overvoltages. On the other hand, overvoltages with a front time of up to 2 μs , frequencies greater than 50 kHz and a time up to half the value of the order of 50 μs are generally considered to be atmospheric surges [27].

Lightning overvoltage is a phase-to-ground or phase-to-phase overvoltage at a given point in the system due to a lightning strike. This overvoltage is characterized by a fast-front overvoltage. While the other types of overvoltages are proportional to the system voltage, overvoltages from lightning strikes depend on system impedances rather than voltage [28].

Electromagnetic transients arise from various events like momentary interruptions, switching, faults and transient voltage/current fluctuations. Artificial intelligence (AI) has demonstrated its effectiveness in addressing power system challenges, including those related to electromagnetic transients within the network [29]. In [30], a method based on time-synchronized high-frequency measurements and using a convolutional neural network was proposed for identifying the causes of electromagnetic transient events. Moreover, a method to classify the causes of transient using support vector machine (SVM) was presented in [31].

In [32], a technique based on SVM was introduced to detect system disturbances and categorize the disturbance waveforms, comparing this approach with the ANN technique. A more recent investigation employs SVMs to detect and categorize transient overvoltages

while mitigating the distortion occurring at signal start and end, which can hinder data processing [33]. Estimation of peak transient overvoltages is explored in [34] using the ANN method.

A combination of approaches—such as integrating ANN-based feature extraction, SVMs and other intelligent methods—has emerged as a viable strategy for resolving challenges in power systems operation [35].

Modeling of elements of electric power systems must consider the range of frequency of the events under study. In what follows, we discuss models of power transformers, surge arresters, transmission lines and circuit breakers.

2.2. Power Transformers

Modeling transformers over a wide frequency range still presents difficulties since transformer inductances are non-linear and frequency-dependent. The losses in the iron and core inductances are non-linear due to saturation and hysteresis and are frequency-dependent from eddy currents in the laminations [36]. During resonance phenomena, resistances greatly influence the maximum voltages of the windings. These high-frequency resistors represent copper and iron losses [37,38]. The distributed capacitances between the turns, winding segments and windings and ground can change the terminal and internal voltages of the transformer due to the resonances they produce [39].

Most models available in computational tools are suitable for evaluating line switching, capacitor switching and transformer energizing [40]. For frequency ranges above 2 kHz, the representation of capacitances is essential. For frequency ranges up to 30 kHz, adding winding capacitances to the ground and between windings is sufficient to reproduce several phenomena. A more detailed representation of the model is necessary for frequencies greater than 30 kHz, containing the modeling of the capacitances between the windings [39].

According to [41,42], models based on lumped parameters can present adequate results for fast transients up to 1 MHz. Therefore, the transformer models used to analyze high-frequency transients can be described by distributed parameters or lumped parameters [40]. Depending on the physical arrangement of the transformer windings, as well as its general design, a range of typical capacitances is adopted for the representation of the terminal-ground values and bushing capacitances, which comprises the range from 1 to 10 nF [39].

One of the leading causes of transformer winding failures is the occurrence of atmospheric discharges and system switching operations, which are transient phenomena that cause voltage surges in the network [3]. In the simulations of these phenomena, the transformer model must consider both the non-linear behavior and the frequency-dependent effects.

According to [43,44], the behavior of some physical attributes of the equipment should be considered for the study of electromagnetic transients: structural characteristics of the core and coils, mutual inductances and self-inductances, stray magnetic fluxes, core magnetic saturation, capacitive effects, and hysteresis. Mathematical modeling of a power transformer is generally divided into two basic approaches in terms of procedures for selecting the model structure and calculating parameters: white-box modeling and black-box modeling [45]. According to [46], the classification also covers another model, known as gray-box.

The white-box modeling is developed from the characteristics of the electrical components that correspond to the physical parts of the equipment's structure [47–50]. These models are not dependent on measurement data, and their parameters have a direct connection with the physical structure of the transformers [51,52].

The level of detail necessary for the construction of the transformer is related to the type of study in which it is inserted. For cases where saturation, residual flux, hysteresis and eddy current losses are important (e.g., inrush currents, ferroresonance), it is essential to propose a more detailed model of the core to obtain more assertive results. For short-circuit cases, for example, a model without the representation of the core can be built [53].

An alternative method is black-box modeling, which can be implemented for both time domain and frequency domain analyses [54,55]. For this model, no prior knowledge about the system or the characteristics of the physical arrangement is used [45]. These models can be used to evaluate current and voltage signals at the transformer terminals [56,57]. Finally, the gray-box modelling is associated with methods and models that can be scaled from a pure physical white-box model to a parameterized black-box model [48,58–61]. Generally, the selection of a suitable representation for a given electromagnetic phenomenon, which may or may not include surge transfer from one winding to another, depends on the frequency range but also on the equipment design and available data [45].

In the analysis of high frequencies, the capacitive effect of the transformer cannot be neglected [62]. It is possible to model the equipment considering the stray capacitances distributed along the windings from concentrated capacitances connected across the transformer terminals. However, the calculation process of these capacitances is not simple, and it becomes a difficult task to find the precise values.

High-frequency transformer models are discussed in [56]. The first model is based on the detailed representation of internal windings, in which large networks of coupled capacitances and inductances are parameterized. These are obtained from discretizing inductances and capacitances of the transformers' own and mutual windings [63,64]. These parameters are obtained through a calculation that requires information from the physical layout and constructive details of the equipment and data from the transformer manufacturers, which are generally unavailable.

The greatest advantage of the model is to allow access to the internal voltages of the windings. It is suitable for calculating the initial voltage distribution along a winding due to impulse excitation; however, it is inappropriate for calculating electromagnetic transients involving the interaction between the system and the equipment. Furthermore, the matrices involved in this type of representation are often extensive, which makes a model impractical for Electromagnetic Transients Program (EMTP).

The other trend in the literature is the models developed from the terminals based on the simulation of characteristics in both the time and frequency domains. These are models with the modeling of the transformer terminals through complex equivalent circuits [65,66]. As a disadvantage, they are not suitable for the application of three-phase transformers.

The representation of transformer windings by electrical parameters is provided by mathematical calculations discussed in [67–69]. The calculation of capacitance to ground is presented in detail in [70]. The determination of inductances can be carried out according to the equations shown in [67,69,71,72]. In the latter, it is also possible to analyze the equation to obtain the resistances of the equipment.

In studies involving transient recovery voltage (TRV), the simulated phenomenon of this paper, it is also necessary to include the bushing and winding capacitances of substation transformers, in addition to the representation of the transfer capacitances between primary and secondary windings [3]. TRV is discussed in greater detail in Section 3. However, for general context, the phenomenon of TRV comprises the resulting voltage between the pole terminals of the circuit breaker after the interruption of the short-circuit current [73,74].

2.3. Surge Arresters

The surge arresters are equipment of great importance for the protection system, and their function is to conduct little or no current for normal operating voltage conditions, or to conduct currents during the occurrence of overvoltages without causing failures. Therefore, the equipment must have a high level of resistance during normal system operation and relatively low resistance during transient overvoltages. In order to elucidate this issue of voltage and current, the literature presents a nonlinear characteristic curve [75]. This behavior is provided in the equipment data sheet from the manufacturer.

In order to shed light on the primary models of surge arresters, a concise literature review is conducted. The traditional model of the device comprises a single nonlinear resistor, represented by a collection of points on the voltage and current characteristic

curve mentioned earlier. However, this static characteristic fails to provide a satisfactory representation of the dynamic behavior.

When examining the constructive aspect of surge arresters, the initial surge protection devices consisted of spark gaps connected in series with silicon carbide (SiC) discs, which serve as nonlinear materials. These spark gaps exhibit high impedance during normal conditions, while the SiC discs are designed to block current flow following an electrical discharge. The V-I characteristic curve of the surge arresters is dependent on the current waveform, whereby faster rise times lead to voltage spikes.

Throughout the years, numerous models have been developed to elucidate frequency-dependent phenomena. In the late 1970s, ref. [76] described the dynamic performance of metal oxide lightning arresters. As reported in this work, lightning is accountable for approximately 30% to 50% of all distribution system outages and a comparable percentage of failures in distribution equipment, as evidenced by the literature.

The metal oxide lightning arresters are composed of a series arrangement of zinc oxide elements with nonlinear resistance. In [77], a straightforward equivalent circuit is introduced to represent the dynamic characteristics of the zinc oxide (ZnO) element. This enables the analysis of the impact of atmospheric discharges on gas-insulated substations using a computational tool, considering different scenarios. When comparing the overvoltage protection performance of the metal oxide device and the conventional one, the former is more suitable for application in gas-insulated substations.

In [78], a method of predicting the operation and performance of metal oxide lightning arresters in power system applications is presented. The analysis covers the V-I characteristic curve when considering low currents for thermal behavior and high currents for response to surges and system disturbances.

The work [79] outlines the process of determining the required parameters for representing a lightning rod made of metal oxide, specifically for conducting transient simulations. In another study [80], they observed a correlation between the voltage peak amplitude and the properties of the zinc oxide (ZnO) used in the metal oxide lightning rod. The material composition has an impact on this peak. The simulations confirmed that a voltage peak of approximately 10% can be attributed to the presence of ZnO in the material.

The literature also presents other models in addition to the conventional one, such as the model by [80], which was obtained in laboratory tests and in the analysis of the micro-structure of the zinc oxide (ZnO) varistor. This model allowed us to verify the need to improve the representation of the ZnO grain boundary, which is responsible for the high non-linearity of the device. In addition, the ZnO grain itself, responsible for the inductive characteristic of the equipment in the high current region, also presented conclusions to improve the representation [80].

In [81], a discussion on models for representing the simplification in [80] is presented. The nonlinear resistance of this model represents the high non-linearity of the device and is determined from its V-I characteristic curve. In order not to need this curve, the IEEE W.G. model 3.4.11 was developed. In this sense, the model only requires knowledge of the value of the residual voltage for the standard impulse of 10 kA and 8/20 μ s, the height of the lightning rod in meters and the number of varistor columns inside the housing [82]. Figure 2 presents an adapted image of the model proposed by [82].

In the context of metal oxide models, ref. [83] presents a set of criteria for determining the parameters of the model. These criteria enable the direct calculation of model parameters using standard data provided in the technical specifications of the devices. To assess the effectiveness of this method, multiple manufacturers were analyzed, covering various applications in medium and high voltages. The results obtained from the ATPDraw software were compared with the tests conducted by the manufacturers, and they demonstrated consistency in the context of isolation coordination studies involving transients.

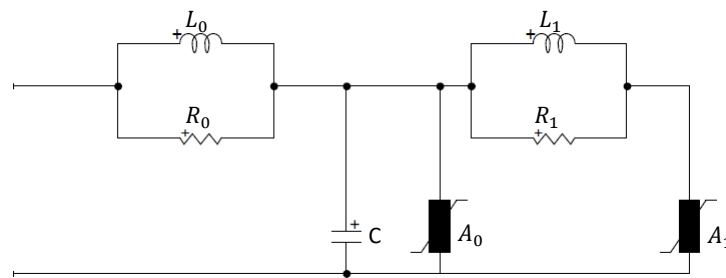


Figure 2. Frequency-dependent IEEE surge arrester model.

However, after performing calculations for the resistances, inductances and capacitance of the filters using (1)–(5), it was found necessary, following the method proposed by [82], to manually adjust the value of inductance L_1 , as well as the nonlinear elements A_0 and A_1 . This adjustment was required in order to fine-tune the response of the model to the residual voltage obtained from an atmospheric pulse with a duration of $8/20 \mu\text{s}$ and an amplitude of 10 kA, as well as for a maneuver pulse with the values provided in the lightning arresters' data sheets [83]. The values for inductances, resistances and capacitance are provided as follows:

$$L_0 = 0.2 \cdot \frac{d}{n} \mu\text{H} \quad (1)$$

$$L_1 = 15 \cdot \frac{d}{n} \mu\text{H} \quad (2)$$

$$R_0 = 100 \cdot \frac{d}{n} \Omega \quad (3)$$

$$R_1 = 65 \cdot \frac{d}{n} \Omega \quad (4)$$

$$C = 100 \cdot \frac{n}{d} \text{pF} \quad (5)$$

where d —height of the surge arresters and n —number of columns of zinc oxide material

In an effort to simplify the IEEE model, ref. [83] developed an alternative model that eliminates the need for manual adjustments to the calculated parameters. This new model's equations do not rely on physical data; instead, they only require the input of the rated voltage, the residual voltage for an atmospheric impulse of 10 kA and the residual voltage for a steep impulse.

Non-frequency-dependent models are suitable for simulations involving low-frequency groups, specifically groups I and II, as specified in Table 2. However, when studying phenomena characterized by high frequencies, such as groups III and IV, it is essential to employ a frequency-dependent model. It is worth noting that a high-frequency model should incorporate the inherent inductance of the device, along with a concentrated inductance in the margin of 1 H/m for grounding cables [75]. For guidelines regarding the representation of metal oxide devices and varistor materials, please refer to Table 4.

Table 4. Guidelines to represent metal-oxide surge arresters.

Model	Group I	Group II	Group III	Group IV
Characteristics	0.1 Hz–3 kHz	60 Hz–20 kHz	10 kHz–3 MHz	100 kHz–50 MHz
Frequency-Dependent V-I Characteristic	Negligible	Negligible	Important	Very Important

2.4. Transmission Lines

Accurately representing the wave propagation in transmission lines is a complex task [84,85]. To achieve precise results in digital simulations, it is crucial to accurately model the system elements based on the corresponding frequency range [16]. This ensures that the phenomena under study are correctly simulated, enabling accurate analysis and results.

Transmission lines, like other equipment, can be modeled either in the time domain or in the frequency domain. However, the nonlinear nature of their elements poses a challenge when representing them in the frequency domain. Therefore, it is generally preferred to develop models for transmission lines in the time domain [86]. Moreover, when analyzing transient phenomena using computational tools, it is essential to represent the system components in the time domain for accurate results.

In the field of transmission line modeling, one of the pioneering time domain models was introduced in [84] by utilizing Bergeron's method. This model is an algorithmic approach capable of simulating electromagnetic transients in discrete or distributed parameter networks. When analyzing shunt connections and switching operations on transmission lines, it is possible to represent them using a cascade of π circuits. Each segment in this model consists of a combination of series and parallel resistors and inductors that take into account factors such as soil and skin effects [87,88].

When it comes to the parameters of transmission lines, they can be represented using either lumped or distributed parameter models. Distributed parameter models take into account the frequency dependence, while constant parameter models do not. By considering the frequency dependence, the system is represented more accurately in relation to its real physical behavior. However, this increased accuracy comes at the cost of higher computational effort.

Another important aspect to note is that poly-phase lines can be modeled in either the modal domain or the phase domain. For transient studies, modal models are commonly used. In these models, the line's n phases can be decoupled by calculating the eigenvalues and eigenvectors of the matrices that describe the line. This decoupling process allows the n phases of the poly-phase line to be treated as individual single-phase lines. This approach simplifies the calculation of electromagnetic transient responses [89,90].

2.4.1. Frequency-Independent Model

In the literature, there are notable models that consider only constant parameters, without frequency dependence. One such model is the Bergeron model, which is closely associated with the method of characteristics. This model is commonly used in situations where a single frequency predominates, such as studies involving impedance evaluated at the fundamental frequency, relay tests or power flow validation.

Another well-known model is the π model, which provides a reasonably accurate representation of the line. This model employs a circuit consisting of a series impedance between the two ends of the circuit and a shunt admittance allocated at each end of the circuit [91]. This structure includes series impedances and shunt admittances as well [92].

2.4.2. Frequency-Dependent Model

To achieve greater accuracy in analyzing a wide range of frequencies, it is necessary to consider distributed and frequency-dependent parameters in the model. Therefore, this section provides a brief literature review of some commonly discussed models over the years.

One notable model is proposed by [90], which employs a transformation matrix to decouple the phase model into the aforementioned modes. In most cases, this matrix remains constant for all frequencies, except for low-frequency ranges and when studying perturbations in parallel lines with different circuits [93]. This model takes into account the frequency dependence of all line parameters, including inductance, capacitance and active resistance [90].

Another well-established model is the universal line model (ULM) introduced by [94]. This model operates in the phase domain and is applicable to various types of line configurations, even in cases where the transformation matrix depends on frequency due to significant differences in modal propagation times. In the ULM, the characteristic admittance and propagation function are determined in the phase domain. Additionally, the propagation function is obtained through the modal model and subsequently fitted in the phase domain for improved accuracy.

Regarding the utilization of computational tools, EMTP-type programs commonly employ the Bergeron models and the model proposed by [90] for constant parameters. However, when considering frequency-dependent parameters, the ULM model is widely implemented in these tools. One of the main advantages of the ULM model is its versatility as it can be utilized for modeling both overhead lines and underground cables, making it highly useful in a variety of scenarios.

It is worth emphasizing that models developed in the modal domain, such as Martí's model [90], yield precise results for symmetric configurations and continuously transposed lines. However, the use of constant transformation matrices is not advisable for non-transposed lines and cables [95]. To provide a summary of the key models in the literature and their specific characteristics, Table 5 is presented.

Table 5. Overview of transmission line models.

Model Characteristics	Constant Parameters	Frequency-Dependent Parameters
Lumped Parameters	Model π	-
Distributed Parameters	Bergeron	Martí and ULM

2.5. Circuit Breaker

The performance of circuit breakers in high-voltage systems plays a crucial role in ensuring the safety and stability of power system operations [96]. Computational tools offer a range of models with varying levels of complexity. The simplest model represents a circuit breaker as an ideal switch that opens when the current passes through zero after a predefined time. However, in gas circuit breakers, the electric arc can be seen as a heat source in a high-speed gas flow [97]. It is important to note that the breaking action of this model is independent of the electric arc itself [98].

Table 6 shows modeling guidelines proposed by [99] for representing circuit breakers in opening operation.

Table 6. Modeling guidelines for circuit breakers.

Opening Operation	Group I 0.1 Hz–3 kHz	Group II 60 Hz–20 kHz	Group III 10 kHz–3 MHz	Group IV 100 kHz–50 MHz
High current interruption	Important only for interruption capability studies	Important only for interruption capability studies	Negligible	Negligible
Current chopping	Negligible	Important only for interruption of small inductive currents	Important only for interruption of small inductive currents	Negligible
Re-strike characteristic	Negligible	Important only for interruption of small inductive currents	Very important	Very important
High-frequency current interruption	Negligible	Important only for interruption of small inductive currents	Very important	Very important

To provide a clearer understanding of the physical nature of the electric arc, particularly in relation to the TRV phenomenon, a brief overview will be presented. The process of interrupting current within the extinguishing chamber can be described in four distinct steps. Initially, the circuit breaker contacts are closed, and the current flows smoothly through the device. When the moving contact begins to separate, the circuit breaker's opening process is initiated, and the current is transferred to the stationary contacts.

As the contacts continue to separate, an electric arc is formed between them, allowing the current to flow across the circuit breaker terminals [100–102]. Simultaneously, a blast of insulating gas is released into the extinguishing chamber, aimed at extinguishing the arc. To ensure successful interruption of the current, the contacts need to be fully open at this stage. As the current approaches zero, the electric arc rapidly loses conductivity during the interruption process. A short time after the current reaches zero, the current circulation is completely interrupted, and the arc is extinguished. However, at this point, the TRV imposed by the electrical network induces a residual voltage across the contacts. If the TRV exceeds the dielectric strength between the contacts, it can result in arc re-ignition and failure of the circuit breaker.

In the 1930s and 1940s, the first tests regarding circuit breakers were conducted and reported in [103,104]. Since then, subsequent researchers have built upon their initial equations and incorporated them into their own models. Several models have been proposed in the literature for circuit breaker implementation. In the case of SF₆-insulated circuit breakers, ref. [105] highlights the significance of the differential equations introduced in [103,104]. Based on these equations, ref. [105] developed a model that incorporates two resistors connected in series. In situations involving high currents, the majority of the arc voltage is governed by Cassie's equation. As the current approaches zero, the portion of the equation from [103] undergoes a modified value, capturing the TRV after the current interruption. At the same moment, the equation from [104] reaches zero.

In [98], various models were presented for analyzing the transient period. One of the simplified models for the device involves an ideal switch that opens when the current passes through zero for the first time. A more advanced model considers the arc as a time-varying resistance or conductance, determined by the device characteristics and breaking current. This model also incorporates the inclusion of the arc in the system if detailed information about it is available. However, it is worth noting that obtaining accurate arc parameters can be difficult. To evaluate the suitability of the circuit breaker, it is essential to consider TRV curves [98].

Another model that is available represents the device as a dynamically changing resistance or conductance, with the value being dependent on the measured voltage and current values. This model differs from the previous one mentioned as it does not require the use of pre-calculated TRV curves. Its primary focus is on short-circuit breaking and switching applications involving inductive currents. Additionally, it is specifically applicable to SF₆-gas-insulated devices [98].

In [106], the devices built need short circuit tests so that the design and manufacture are carried out with greater assertiveness. In order to develop the electric arc model, it is crucial to consider the information regarding the arc column, cooling and dielectric strength during the opening of the contacts. When mechanical circuit interruption occurs, the plasma column is ionized and the arc must be extinguished when the current passes zero.

According to [107], the parameters of the TRV envelope defined in the standards specified in Section 3.1 are determined based on the ideal circuit breaker circuit without considering the influence of the arc. Therefore, the electric arc model is often disregarded in studies of this phenomenon [108].

3. Transient Recovery Voltage

In the early 20th century, studies began to investigate the TRV phenomenon. During this period, several publications emerged that focused on determining the characteristics of TRV in power systems [109–112]. One of the notable findings was that faults could

result in high initial RRRV at current zero, which could potentially cause the arc in the circuit breaker to reignite before the full system recovery voltage could manifest [113]. Furthermore, in [114], the author examined how the interrupting capacity of a circuit breaker is influenced by the natural voltage oscillations of the system when current is interrupted after the instant of current zero. This phenomenon corresponds to the difference in voltage obtained by subtracting the voltage to ground on one side of the breaker from the voltage to ground on the other side during an opening operation [115]. Recent research indicates that TRV investigations are being conducted within grid-connected systems with voltages exceeding 15 kV [116–118].

When it comes to extinguishing the electric arc, there are several types of circuit breakers commonly used in electrical systems, including Sulphur Hexafluoride (SF₆), oil-insulated, compressed-air-insulated and vacuum-insulated circuit breakers. In the case study, the circuit breakers being analyzed are SF₆-insulated, and, therefore, a brief characterization of SF₆ circuit breakers is provided below.

SF₆ gas began to be used as an insulating medium in transformers in the 1930s, a few years after its synthesis. In addition to having a greater dielectric strength than air, SF₆ gas has a high heat transfer capacity and low ionization temperature, factors that make it an excellent arc-extinguishing medium. Thus, about a decade after its use in transformers, SF₆ gas began to be implemented in circuit breakers as an insulating medium and arc flash extingisher [119,120].

During fault conditions in an electrical system, it is crucial that the circuit breaker maintains its current interruption capacity and continues to function effectively. The proper operation of the circuit breaker is essential in minimizing the impact of a short circuit on the overall system behavior. This becomes particularly important when the network is exposed to extreme fault conditions. Ensuring the circuit breaker's successful operation helps safeguard the system and prevents damage or disruption caused by faults.

The TRV refers to the difference in phase-to-ground voltages at each terminal of a circuit breaker. It is characterized by a high-frequency component that decays within microseconds but gives rise to RRRV [121]. RRRV is a serious transient phenomenon that can cause interruptions in the power supply to customers and result in maintenance costs for power utilities [122].

During the interruption of a fault, the electric arc in a circuit breaker quickly loses its conductivity as the current approaches zero. At this point, a voltage response known as TRV is generated. TRV is a result of the stress on the insulation gap and the arcing that occurs within the interrupting medium. To ensure that the circuit breaker is not overwhelmed by TRV, it must be capable of withstanding the generated voltage response without any detrimental effects on its operation or insulation [123].

After the current is extinguished, the internal mechanisms try to recover the dielectric characteristics of the insulating medium [124]. During this same period, the voltage request between the contacts acts in the opposite direction, which may cause a re-ignition. During the interruption process, the arc rapidly loses its conductivity as the current approaches zero [123]. After this period, TRV occurs, which, in other words, consists of a power system response to a sudden change in the network topology, with high frequency and amplitudes.

According to [123], the nature of TRV depends on the characteristic of the investigated system, whether it is predominantly capacitive, resistive or inductive. According to [125], in power systems of inductive predominance, the interruption coincides with the maximum time of the voltage expressed by the sinusoid. As the TRV depends on the system conditions and the parameters involved in the circuit, it is important that they are studied for circuit breaker specifications [123].

To prevent the re-ignition process from occurring, the dielectric recovery must be greater than the voltage request between its contacts. When the contacts are already farther apart, the maximum TRV value that is capable of not exceeding the dielectric capacity of the insulating medium must be calculated and analyzed. Thus, studying and analyzing the TRV phenomenon is important in order to ensure that the circuit breaker's electrical

insulation limits are not violated since arc re-ignitions can drastically damage the circuit breaker's operation and functionality [126].

Concerning the events that can cause severe damage to the circuit breaker, it is possible to cite faulty terminals and short-line faults. According to [127], the growth in short-circuit currents of power systems motivated the study of short-line faults. In [128], there are two recovery voltage regions of important analysis. The first region comprises up to 100 μ s or 200 μ s and the second region up to 1000 μ s. During the first microseconds of the first region, high RRRV may produce thermal failure, in addition to dielectric failure. In the second region, it is common for waves reflected from the lines connected to the faulty bus to return to the circuit breaker. This reflection results in an increase in the RRRV. As mentioned in [126], this can potentially lead to dielectric failure.

3.1. Normative Considerations

The choice in circuit breakers for a system is generally based on the required short-circuit breaking capacity. However, each contact opening results in a TRV that can affect the dielectric characteristic of the equipment, although currents may be less than the rated short-circuit current [129].

To ensure the reliability and safety of the power system, it is crucial to have accurate knowledge of the specified values for a circuit breaker. This is important because the circuit breaker can be exceeded in terms of its short circuit breaking capacity and its ability to withstand TRV. The short circuit breaking capacity of a circuit breaker is determined by comparing the specified values, which indicate the maximum current it can handle, with the permissible values for the recovery voltage that occurs after the contacts are opened.

This section focuses on discussing the regulatory aspects related to the short-circuit current breaking capacity of a circuit breaker. It also explores the potential standardized criteria for stress analysis. To facilitate comprehension of the normative parameters mentioned in this section, it is important to provide an explanation of certain concepts related to circuit breakers.

According to [130], the first pole-to-clear factor is defined as the ratio of rms voltage between the faulted phase and unfaulted phase and phase-to-neutral voltage with the fault removed. This concept takes into account the non-simultaneity of the interruption of the arc in the three phases. Furthermore, the most severe oscillatory or exponential recovery voltages tend to occur across the first pole to open of a circuit breaker interrupting a three-phase ungrounded symmetrical fault at its terminal when the system voltage is maximum [131].

After the pole opening, the voltage wave has a high amplitude and an RRRV that have their values established in the standards [132,133], which also provide for studies for short-line faults, terminal faults and openings with the phases not synchronized. In the case of terminal faults, different short circuit levels are foreseen in relation to the breaking capacity of the circuit breaker.

As for the waveform, the TRV can differ in some categories, such as exponential, oscillatory and triangular, depending on the power system response [134,135]. For the circuit breaker interruption scenario in substations, the waveform obtained is exponential, with an over-damped characteristic [124].

3.2. Circuit Breaker Override Analysis by TRV

To establish reference parameters for TRV values, envelope curves have been developed to indicate the capability of the investigated circuit breaker. These envelope curves are specified in standards such as [131–133]. The standard [133] standard [118] defines the TRV envelope, which can be represented by two or four parameter curves. On the other hand, according to the standard [132], TRV behavior varies in systems with voltage equal to or greater than 100 kV. Initially, there is a high RRRV, and, later, this rate is reduced [131].

The TRV waveform, in the case of significant short-circuit currents, can be represented by an envelope defined by four parameters. However, for systems with voltages

below 100 kV, when the short-circuit current is relatively low compared to the maximum short-circuit current and supplied by transformers, the resulting waveform can be approximated by a two-parameter envelope [121]. Figure 3, adapted from [123], illustrates these envelope curves.

The graph highlights the parameters that represent important voltage values and their corresponding time periods. The parameter u_1 denotes the first reference voltage reached, and its corresponding period is denoted by t_1 . The parameter u_c represents the maximum voltage reached, and its corresponding period is denoted by t_2 . In the case of the four-parameter envelope curve, there is an additional parameter u_c that represents the final voltage reached, and its corresponding period is denoted by t_3 . Both envelope curves also involve auxiliary parameters that account for time delays in the analysis.

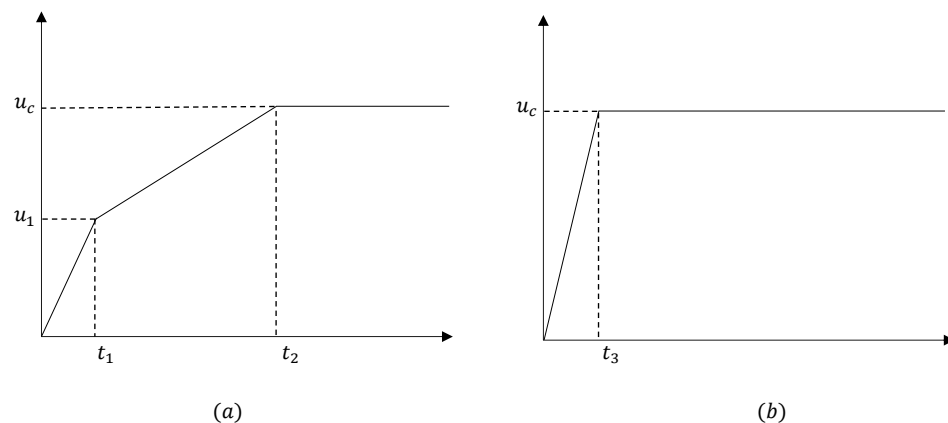


Figure 3. Envelope defined to: (a) four parameters, (b) two parameters.

If the envelope limits are exceeded during the operation to clear a short circuit, it is necessary to either replace the circuit breaker being investigated or implement mitigation methods to address the issue [136]. For instance, the research conducted in [137] explored the use of supercapacitors for mitigating TRV.

The standard [133] specifies the parameters for the standardized envelope tests at various levels of short-circuit currents, namely 10%, 30%, 60% and 100% of the rated short circuit breaking capacity. As the short-circuit currents decrease, the envelope capacities increase. According to [138], circuit breakers with a rated voltage below 100 kV are classified into two classes: S1 and S2. A circuit breaker belonging to class S1 is designed for cable systems, while a circuit breaker in class S2 is designed for overhead line systems.

The oscillatory or exponential recovery voltages typically occur when the first pole of a circuit breaker opens during the interruption of a three-phase symmetrical fault without grounding at its terminals, while the system voltage is at its maximum [131]. In the case of a three-phase ungrounded fault, the first pole factor is denoted by a constant of 1.3 for effectively grounded systems. However, for ungrounded systems, this first pole factor is assumed to be 1.5 [121]. The TRV characteristic curve tends to be complex, which highlights the importance of utilizing computational tools to aid in its analysis.

3.3. Computational Methods for TRV Analysis

Due to the high complexity of electrical systems, manually solving the differential equations that describe the dynamic behavior of the power system becomes impractical. Instead, the use of computational tools offers a more practical and effective solution for representing the components of the electrical network and obtaining accurate results. In digital offline simulation, the primary objective is to develop suitable methods for analyzing future phenomena. However, while power system variables are continuous, computational simulations are inherently discrete. This poses a major challenge of developing appropriate methods to solve differential and algebraic problems at discrete points in the simulation [139].

Numerical solution techniques based on nodal analysis were introduced in [84,89,140,141], enabling the calculation of electromagnetic transients. Within the software category for simulating electromagnetic transients, EMTP (Electromagnetic Transients Program) stands out. Developed by BPA (Bonneville Power Administration), EMTP offers various models for representing power system equipment, such as transmission lines, transformers, surge arresters and circuit breakers [142]. These models provide detailed and complex representations of transient phenomena in power systems.

4. Transient Recovery Voltage Simulation

The TRV to which a circuit breaker is subjected depends on the type of fault, the location of the fault and the characteristics of the network [143]. In that sense, to complement the literature review focusing on TRV requests imposed on circuit breakers, a set of computational simulations was performed using parameters from a real power substation in southern Brazil. The simulated scenarios aim to evaluate the supportability of circuit breakers, for maximum voltage and rate-of-rise of recovery voltage during the occurrence of a TRV, considering the envelope standardized by the IEEE [132,133].

The characteristics of the power substation, the simulation parameters and the analysis of results are presented in this section.

4.1. Simulated Case

To assess the supportability of the circuit breakers of the substation considered in this case study, simulations were carried out in the EMTP-RV software using real data. The simulations involved three-phase grounded and ungrounded faults. The substation operates at a voltage level of 230 kV. The one-line diagram of the power substation used in the computer simulations for TRV analysis is presented in Figure 4. The faults simulated for TRV analysis in circuit breaker CB11 were located at FL1 and FL2, while FL3 represented the fault location for circuit breaker CB1.

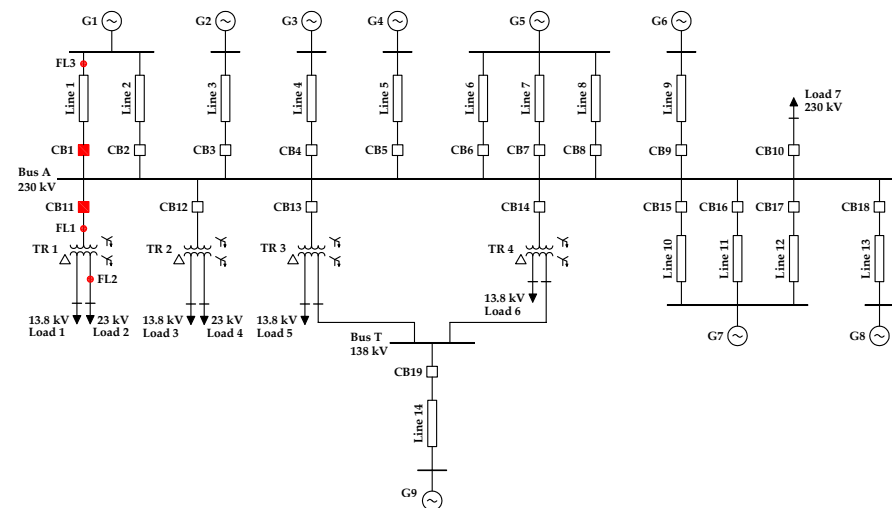


Figure 4. Simplified one-line diagram of the substation.

The characteristics of the simulated system are presented in this subsection. In the lines, the EMTP wide band model was used, which is the most accurate model for time domain simulations of lines for a large band of frequencies [144]. The lines are arranged in two configurations, as shown in Figure 5. Lines 1 to 13 use configuration 1, with Cardinal-type phase cables, and line 14 uses configuration 2, with Lynx-type cables. The overhead ground wires on all lines are of the Alumosteel 1/0 20% IACS type. Table 7 presents the test system line lengths.

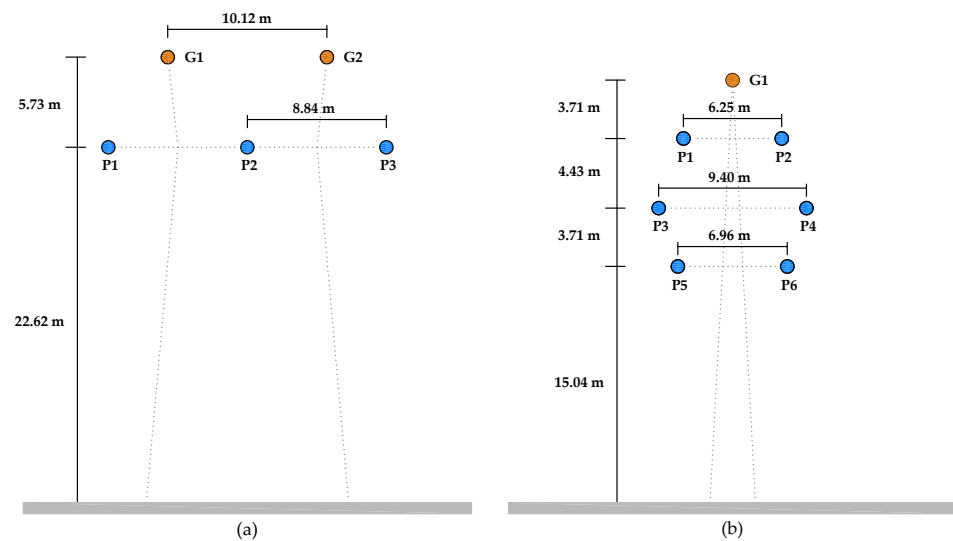


Figure 5. Tower configuration type: (a) configuration 1, (b) configuration 2.

Table 7. Line data.

Line	Length (km)	Line	Length (km)
1	17.20	8	23.00
2	14.82	9	102.00
3	38.50	10	13.00
4	46.90	11	13.00
5	23.60	12	13.00
6	23.00	13	9.00
7	23.00	14	22.90

Table 8 presents the data of the equivalent loads connected to the substation. Table 9 shows information about Thévenin's equivalent systems viewed from the substation, where Z_{th_0} , Z_{th_1} and Z_{th_2} denote the equivalent zero, positive and negative sequence impedances, respectively. Additionally, Table 10 presents information about the types of connections, nominal voltages (primary, secondary and tertiary), nominal powers and electrical parameters (resistance and reactance in per unit) for three-phase transformers with three windings.

Table 8. Load data.

Load	P (MW)	Q (MVar)
1–3–5–6	0.14	0.06
2–4	42.75	14.05
7	49.80	16.50

Table 9. Equivalent systems.

Sourcer	V_{th} (kV)	Z_{th_0} (Ω)	$Z_{th_1} = Z_{th_2}$ (Ω)
G1	230	2.260 + j 6.478	29.805 + j 308.446
G2	230	2.628 + j 17.873	4.556 + j 33.791
G3	230	2.951 + j 32.725	19.448 + j 128.644
G4	230	1.073 + j 26.137	10.672 + j 98.312
G5	230	1.117 + j 7.262	0.405 + j 7.777
G6	230	4.622 + j 46.055	18.259 + j 103.168
G7	230	0.278 + j 3.787	0.621 + j 9.132
G8	230	0.158 + j 0.397	14.668 + j 38.997
G9	230	0.531 + j 10.139	12.098 + j 133.193

Table 10. Transformer data.

Transformer	1	2	3	4
Vector group	YNyn0d1	YNyn0d1	YNyn0d1	YNyn0d1
Voltage (kV)	230/23/13.8	230/23/13.8	230/138/13.8	230/138/13.8
Rated (MVA)	50	50	225	225
R_{12} (p.u.)	0.178	0.733	0.102	0.102
R_{13} (p.u.)	1.601	3.649	0.287	0.287
R_{23} (p.u.)	1.539	3.564	0.305	0.305
X_{12} (p.u.)	28.520	27.200	4.360	4.360
X_{13} (p.u.)	49.280	50.190	17.920	17.920
X_{23} (p.u.)	16.800	17.110	11.660	11.660

4.2. Methodological Procedures and Simulation Data

In [131], a guide for the application of TRV for AC high-voltage circuit breakers is presented. In the TRV calculation process, circuit constants are required for each element within the system. Typically, only inductances and capacitances are considered, while resistance is neglected [131]. This guide offers valuable insights and contributions to the analysis of TRVs in circuit breakers. Additionally, it provides a range of typical capacitance values for various equipment found in a power substation. These capacitances pertain to the modeling of equipment such as circuit breakers, disconnect switches, bus bars, capacitive and inductive potential transformers.

The stray capacitances of equipment present in substations can be modeled using typical values found in the IEEE Std. C37.011, as demonstrated in a recently published article [145]. In the simulations we present, three capacitance values for the equipment were selected from the range provided in [131]. Table 11 shows these capacitance values, denoted as C_{min} , C_{avg} and C_{max} , representing the minimum, average and maximum values, respectively.

Table 11. Typical equipment capacitances.

Equipments	C_{min} (pF)	C_{avg} (pF)	C_{max} (pF)
Circuit Breaker	50	150	250
Disconnect Switches Closed	60	130	200
Disconnect Switches Open	30	80	130
Surge Arresters	80	100	120
Capacitive Voltage Transformer	3000	7750	12,500
Inductive Instrument Transformer	75	167.5	260
Bus Capacitance	8.2	13.1	18

To perform TRV analysis using EMTP-RV, the envelope utilized for analysis is based on the curves provided in [132,133] for circuit breakers rated above 100 kV with effective grounding. This analysis involves four parameters, as illustrated in Figure 3. Among the nominal voltage ranges available in the software, a voltage of 245 kV was selected for the analysis. The investigated circuit breaker has a nominal current of 40 kA, and its breaking current capacity is approximately 34.9 kA, which is approximately 85% of the rated current value. According to the [133] standard, which defines the parameters of the standardized envelope for tests conducted at currents ranging from 10% to 100% of the circuit-breaker-rated short-circuit, the software performs an interpolation between 60% and 100% to obtain the parameters associated with the envelope.

Table 12 presents the parameters derived from standards [132,133] that were utilized in the simulations for ungrounded three-phase faults. The parameters u_1 , t_1 , u_c and t_2 have been discussed in Section 3.2. The RRRV (rate of rise of recovery voltage) represents the initial slope of the rated TRV and is calculated by dividing the TRV by the time it takes for the TRV to reach its peak value [146]. The parameters u' and t_d denote the peak voltage and

time delay of the TRV, respectively. The term k_{pp} represents the first-pole-to-clear factor, while k_{af} signifies the amplitude factor.

Table 12. Parameters of envelope in EMTP-RV—ungrounded three-phase faults.

Parameters of Envelope	Standard IEC	Standard IEEE
u_1	195.04 kV	195.04 kV
t_1	87.69 μ s	87.69 μ s
u_c	372.2 kV	372.2 kV
t_2	392.74 μ s	329.53 μ s
RRRV	2.224 kV/ μ s	2.224 kV/ μ s
u'	97.52 kV	97.52 kV
t_d	2 μ s	2 μ s
k_{pp}	1.3 p.u.	1.3 p.u.
k_{af}	1.43 p.u.	1.43 p.u.

Based on Table 12, there is a discrepancy in the value of parameter t_2 , which represents the duration corresponding to the maximum envelope stress. Therefore, through computer simulations, it will be feasible to examine whether the stress behavior will affect or not the results by observing any deviation in the envelope displacement when compared to another.

4.3. Results and Analysis

To facilitate comprehension and analysis, the simulations were divided into three scenarios. In these scenarios, three-phase faults were simulated within a time frame of 100 μ s, where the fault occurs at the instant of maximum voltage in phase-a for a cosine function. The circuit breaker is then opened at 200 μ s. As stated in [126], TRV considerations typically encompass the time period up to 100 μ s following the circuit breaker opening.

Additionally, during the conducted simulations, three capacitance values (C_{min} , C_{avg} and C_{max} , as listed in Table 11) were employed for the models of substation equipment in each scenario and for each type of fault. The evaluation of circuit breaker supportability took into account the standardized envelope provided by the IEEE [132] and the IEC [133].

4.3.1. Scenario 1

In scenario 1, the circuit breaker CB11 opens in response to a three-phase grounded terminal fault or a three-phase ungrounded terminal fault occurring on the high-voltage side of the transformer. This fault location is illustrated as FL1 in Figure 4.

Regarding the TRV peak, Table 13 displays the results for the highest voltage peak in one of the three phases: a, b or c. The respective letter in parentheses indicates the phase corresponding to the voltage values. According to Table 12, the maximum voltage value u_c is 372.2 kV for both the IEC and IEEE envelopes. Comparing this value with the results presented in Table 13, it is evident that the TRV in phase b exceeds the capability of circuit breaker CB11 for a three-phase ungrounded fault, regardless of the minimum, average or maximum capacitance values. The most severe condition occurs when considering the minimum capacitance value, with a TRV peak of 961.40 kV. On the other hand, it is observed that the TRV does not surpass the capacity of the circuit breaker for a three-phase grounded fault. In this case, the TRV in phase c is equal to 265.84 kV for the maximum capacitance value.

Table 12 provides the maximum RRRV value, determined by the ratio u_1/t_1 , which is equal to 2.224 kV/ μ s. Upon comparing this value with the results in Table 13, it is evident that the capacity of the circuit breaker is not exceeded in any of the simulated conditions. The value that comes closest to the maximum RRRV limit is 2.056 kV/ μ s, observed for a three-phase ungrounded fault when considering the minimum capacitance value.

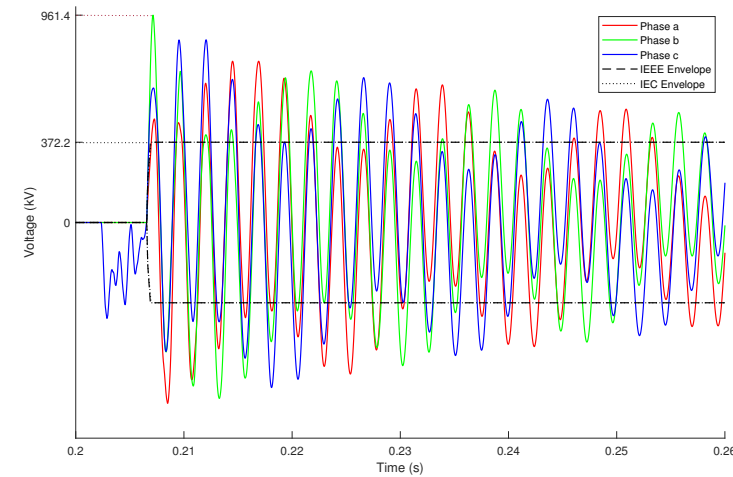
Table 13. Simulation results for scenario 1.

Fault Location	Fault Type	C_{min}		C_{avg}		C_{max}	
		TRV Peak (kV)	RRRV (kV/ μ s)	TRV Peak (kV)	RRRV (kV/ μ s)	TRV Peak (kV)	RRRV (kV/ μ s)
FL1	3 ϕ -G	263.51 (c)	0.556	265.18 (c)	0.532	265.84 (c)	0.529
	3 ϕ -U	961.40 (b)	2.056	908.09 (b)	1.888	860.79 (b)	1.642

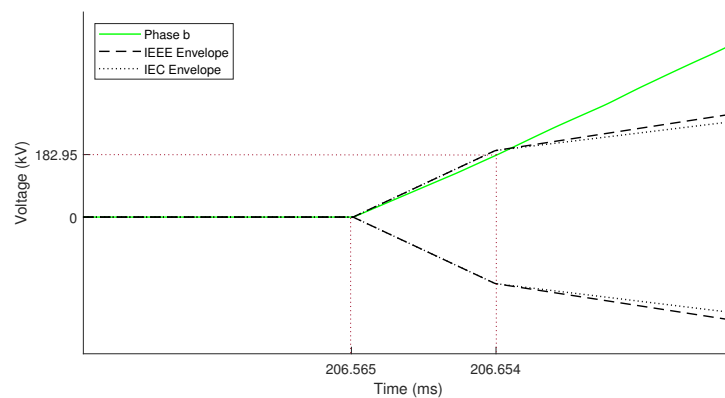
Figure 6 illustrates the maximum voltages in the phases, with a specific focus on the envelope and the voltage in phase b. By referring to Figure 6b, the RRRV can be determined using the times t_f and t_i , along with the voltages u_f and u_i , according to (6):

$$RRRV_{FL1\ 3\phi-U} = \frac{u_f - u_i}{t_f - t_i} = \frac{u_1}{t_1} = \frac{182.95\text{ kV} - 0}{206.565\text{ ms} - 206.654\text{ ms}} = \frac{182.95\text{ kV}}{89\ \mu\text{s}} \quad (6)$$

$$RRRV_{FL1\ 3\phi-U} = 2.056\text{ kV}/\mu\text{s}$$



(a)



(b)

Figure 6. Three-phase ungrounded terminal fault on the high-voltage side of the transformer in FL1: (a) maximum voltages in the phases; (b) highlight of envelope and voltage in phase b.

4.3.2. Scenario 2

In scenario 2, the circuit breaker opens in response to a three-phase grounded terminal fault and a three-phase ungrounded terminal fault occurring on the low-voltage side of the transformer. These fault locations are indicated as FL2 in Figure 4.

In a similar analysis to scenario 1, when comparing the value of $u_c = 372.2$ kV from Table 12 with the results provided in Table 14, it is evident that the TRV does not surpass the capacity of circuit breaker CB11 in any of the simulated conditions. Moreover, upon evaluating the RRRV values presented in Table 14 and comparing them to the RRRV value of 2.224 kV/ μ s from Table 12, one can observe that the capacity of the circuit breaker is not exceeded.

Table 14. Simulation results for scenario 2.

Fault Location	Fault Type	C_{min}		C_{avg}		C_{max}	
		TRV Peak (kV)	RRRV (kV/ μ s)	TRV Peak (kV)	RRRV (kV/ μ s)	TRV Peak (kV)	RRRV (kV/ μ s)
FL2	3 ϕ -G	364.39 (b)	0.055	362.82 (a)	0.046	366.86 (a)	0.046
	3 ϕ -U	364.78 (c)	0.054	362.92 (c)	0.046	361.29 (a)	0.043

Figure 7 shows the maximum voltages in the phases, with a specific focus on the envelope and the voltage in phase a. By referring to Figure 7b, the RRRV for a three-phase grounded fault and maximum capacitance can be determined using the graph and Equation (7):

$$RRRV_{FL2\ 3\phi-G} = \frac{u_f - u_i}{t_f - t_i} = \frac{u_1}{t_1} = \frac{-4.14\text{ kV} - 0}{208.24\text{ ms} - 208.33\text{ ms}} = \frac{-4.14\text{ kV}}{90\ \mu\text{s}} \quad (7)$$

$$RRRV_{FL2\ 3\phi-G} = -0.046\text{ kV}/\mu\text{s}$$

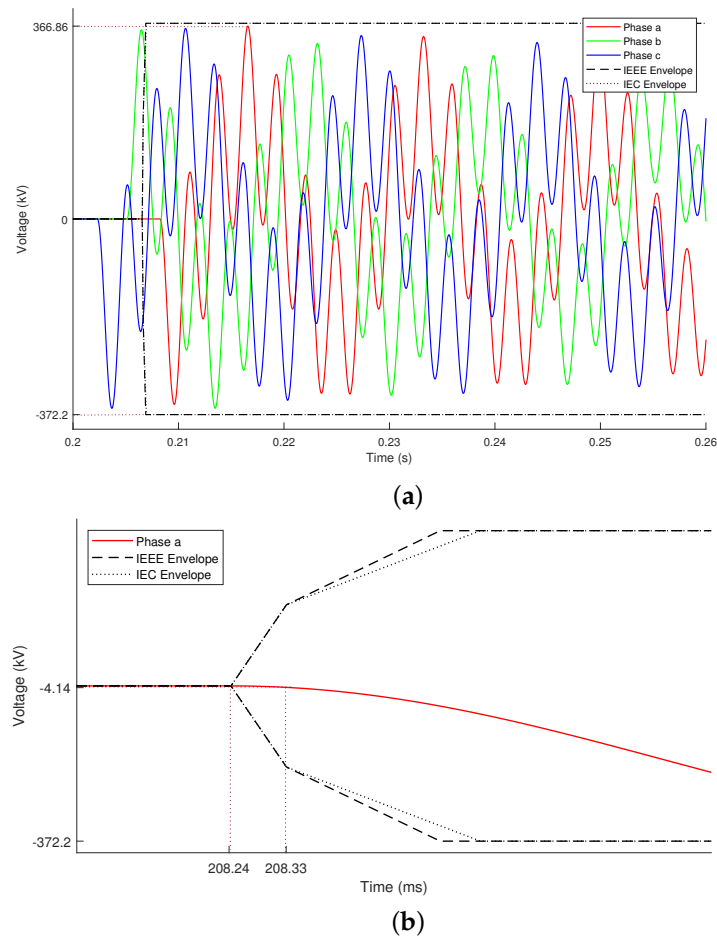


Figure 7. Three-phase grounded terminal fault on the low-voltage side of the transformer in FL2: (a) maximum voltages in the phases; (b) highlight of envelope and voltage in phase a.

4.3.3. Scenario 3

In scenario 3, the circuit breaker opens due to three-phase grounded short-line fault and three-phase ungrounded short-line, shown in Figure 4 as FL3. Similar to the previous scenarios, analyzing the results presented in Table 15, with TRV = 372.2 kV and RRRV = 2.224 kV/μs from Table 12, it is observed that the capacity of circuit breaker CB1 is not exceeded for both TRV peak and RRRV in any of the simulated conditions.

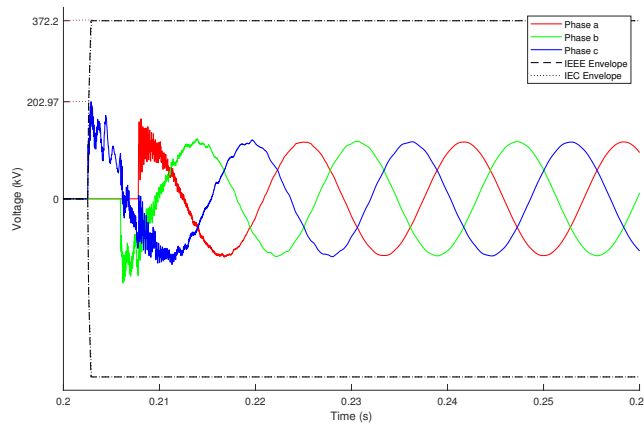
Table 15. Simulation results for scenario 3.

Fault Location	Fault Type	C_{min}		C_{avg}		C_{max}	
		TRV Peak (kV)	RRRV (kV/μs)	TRV Peak (kV)	RRRV (kV/μs)	TRV Peak (kV)	RRRV (kV/μs)
FL3	3φ-G	194.73 (c)	1.171	199.02 (c)	1.459	200.36 (c)	1.142
	3φ-U	188.37 (c)	1.168	198.19 (c)	1.155	202.97 (c)	0.849

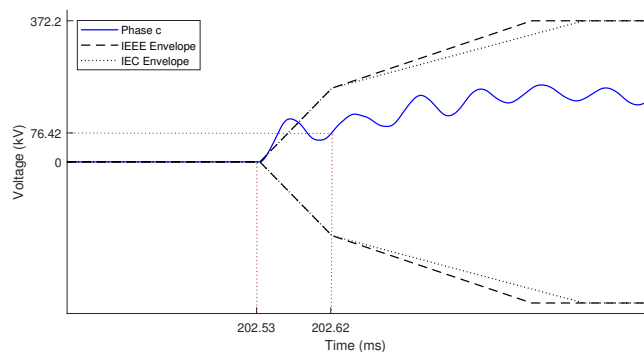
Figure 8 illustrates the maximum voltages in the phases, with a specific focus on the envelope and the voltage in phase c. By referring to Figure 8b, the RRRV for a three-phase ungrounded fault and maximum capacitance can be determined using the graph and Equation (8):

$$RRRV_{v FL3 3\phi-U} = \frac{u_f - u_i}{t_f - t_i} = \frac{u_1}{t_1} = \frac{76.42 \text{ kV} - 0}{202.62 \text{ ms} - 202.53 \text{ ms}} = \frac{76.42 \text{ kV}}{90 \mu\text{s}} \quad (8)$$

$$RRRV_{v FL3 3\phi-U} = 0.849 \text{ kV}/\mu\text{s}$$



(a)



(b)

Figure 8. Three-phase grounded short-line fault in FL3: (a) maximum voltages in the phases; (b) highlight of envelope and voltage in phase c.

The $RRRV_v$, obtained from the graph in Figure 8b, was calculated with a $\Delta t = 202.62 \text{ ms} - 202.53 \text{ ms} = 90 \text{ } \mu\text{s}$. Note that the analysis is performed for a $\Delta t = 202.56 \text{ ms} - 202.534 \text{ ms} = 26 \text{ } \mu\text{s}$, as shown in Figure 9. Based on this, a new $RRRV_n$ can be calculated using Equation (9).

$$RRRV_{n \text{ FL3 } 3\phi-U} = \frac{u_f - u_i}{t_f - t_i} = \frac{u_1}{t_1} = \frac{100 \text{ kV} - 0}{202.56 \text{ ms} - 202.534 \text{ ms}} = \frac{100 \text{ kV}}{26 \text{ } \mu\text{s}} \quad (9)$$

$$RRRV_{n \text{ FL3 } 3\phi-U} = 3.846 \text{ kV}/\mu\text{s}$$

The result reveals that the $RRRV_n$ exceeds the capability of circuit breaker CB1 for a three-phase ungrounded fault.

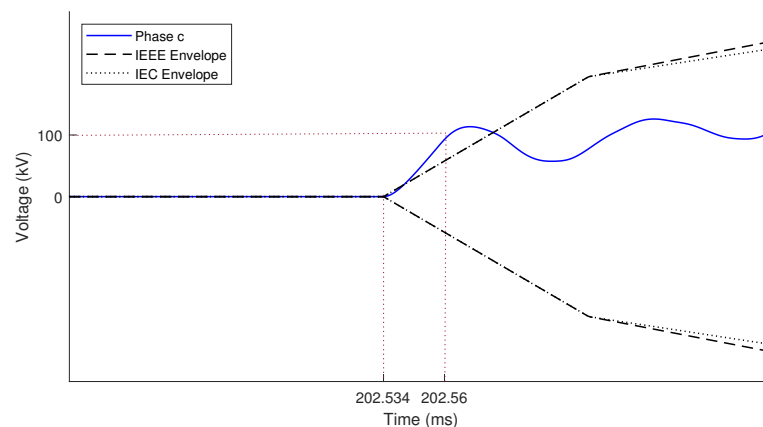


Figure 9. Highlight of envelope and voltage in phase c for $\Delta t = 26 \text{ } \mu\text{s}$.

5. Conclusions

The TRV analysis is a study aimed at verifying the ability of a circuit breaker to withstand network faults. The amplitude and rate of rise of the TRV play crucial roles in the successful operation of high-voltage circuit breakers. Recognizing the significance of TRV studies, this work conducted a comprehensive literature review on the topic. The review revealed the complexity associated with representing certain components of the network as their characteristics vary depending on the frequency of the phenomenon under study.

In the context of the analyzed power substation, the simulation results revealed that variations in the capacitance values used to model the substation equipment have a significant impact on the TRV and RRRV values. However, this sensitivity was observed primarily in the case of a three-phase ungrounded terminal fault occurring on the high-voltage side of the transformer, particularly when the fault was closer to the circuit breaker. Given that capacitance is typically an unknown parameter, selecting an appropriate capacitance value during the modeling becomes crucial to ensure that the obtained results align with the transformer's characteristics.

For scenario 1, it was found that the TRV peak exceeded the capacity of the CB11 circuit breaker by almost three times, proving to be the most critical condition for eliminating a three-phase ungrounded terminal fault on the high-voltage side of the transformer. Regarding scenario 3, the TRV peak remained between the upper and lower limits of the envelopes. Although the analysis of this scenario did not indicate equipment exceeding its capacity in terms of amplitude, when analyzing the time range between 202.56 ms and 202.534 ms, it can be observed, either through calculation or graphical inspection, that the interrupting capacity of the circuit breaker was exceeded by the RRRV. This observation emphasizes the importance of analyzing the TRV in instants immediately after the opening of circuit breaker poles rather than solely focusing on the specific time instants established in the IEEE and IEC standards.

It is important to note that evaluating the circuit breaker's ability to withstand TRV based solely on amplitude is not always conclusive. The outcome also depends on the

switching behavior of the equipment connected to the substation at the time of the fault. Additionally, it is important to note that the results are applicable specifically to the examined power substation. When assessing different substations, it is essential to account for the wide-ranging equipment characteristics present in each individual substation. Nevertheless, the comprehensive literature review and the resulting findings can offer significant guidance to researchers in this field.

Author Contributions: Conceptualization, E.F.L., A.P.d.M., M.R. (Maicon Ramos), R.F. and M.R. (Mariana Resener); methodology, E.F.L., A.P.d.M., M.R. (Maicon Ramos), R.F. and M.R. (Mariana Resener); investigation, E.F.L., A.P.d.M., M.R. (Maicon Ramos), R.F. and M.R. (Mariana Resener); writing—original draft preparation, E.F.L. and M.R. (Mariana Resener); writing—review and editing, V.C.B.; supervision, R.F. and M.R. (Mariana Resener); project administration, T.M., V.C.B., R.C., H.F. and C.C.; funding acquisition, T.M. and V.C.B. All authors have read and agreed to the published version of the manuscript.

Funding: This study was financed in part by the Coordenação de Aperfeiçoamento de Pessoal de Nível Superior—Brasil (CAPES)—Finance Code 001. The authors thank the Electric Sector Research and Development Program, through the project PD-05785-2119/2021: “Computer tool of the study, analysis and diagnosis of very fast transients in power transformers”, regulated by the National Electric Energy Agency—ANEEL, in partnership with CPFL Transmission. The authors also thank the technical and financial support of the Conselho Nacional de Desenvolvimento Científico e Pessoal (CNPq), Federal University of Santa Maria (UFSM), Programa de Pós-Graduação em Engenharia Elétrica (PPGEE), Instituto de Redes Inteligentes, Instituto Nacional de Ciência e Tecnologia em Geração Distribuída (INCT-GD) and Federal University of Rio Grande do Sul (UFRGS).

Conflicts of Interest: The authors declare no conflict of interest.

References

1. Wu, Y.K.; Tan, W.S.; Chiang, Y.S.; Huang, C.L. Planning of Flexible Generators and Energy Storages under High Penetration of Renewable Power in Taiwan Power System. *Energies* **2022**, *15*, 5224. [\[CrossRef\]](#)
2. Gitelman, L.; Kozhevnikov, M. Energy Transition Manifesto: A Contribution towards the Discourse on the Specifics Amid Energy Crisis. *Energies* **2022**, *15*, 9199. [\[CrossRef\]](#)
3. Greenwood, A. *Electrical Transients in Power Systems*; OSTI: New York, NY, USA, 1991.
4. Chowdhuri, P. Calculation of Series Capacitance for Transient Analysis of Windings. *IEEE Trans. Power Deliv.* **1987**, *2*, 133–139. [\[CrossRef\]](#)
5. Bewley, L. Traveling waves on transmission systems. *Trans. Am. Inst. Electr. Eng.* **1931**, *50*, 532–550. [\[CrossRef\]](#)
6. Heller, B.; Veverka, A. *Surge Phenomena in Electrical Machines*; Iliffe: Prague, Czech Republic, 1968.
7. Rüdénberg, R. Electrical Shock Waves in Power Systems. In *Electrical Shock Waves in Power Systems*; Harvard University Press: Cambridge, MA, USA, 2013.
8. Degeneff, R.; Grigsby, L. *Transient-Voltage Response*; Electric Power Transformer Engineering; CRC Press: Boca Raton, FL, USA, 2007.
9. Martinez-Velasco, J.A. *Transient Analysis of Power Systems: Solution Techniques, Tools and Applications*; John Wiley & Sons: Hoboken, NJ, USA, 2014.
10. Pant, D.C.; Kaur, G.; Sharma, S. Study and Analysis of Temporary and Transient Overvoltages in a Wind Farm. *IJEETC* **2015**, *1*, 28–32.
11. Dufournet, D.; Montillet, G. Transient recovery voltages requirements for system source fault interrupting by small generator circuit breakers. *IEEE Trans. Power Deliv.* **2002**, *17*, 474–478. [\[CrossRef\]](#)
12. Waruna, C.; Bruno, B.; Jeff, C. Effects of phase-shifting transformers and synchronous condensers on breaker transient recovery voltages. *Electr. Power Syst. Res.* **2008**, *79*, 466–473.
13. Soloot, A.H.; Hoidalén, H.K. Upon The Impact of Power System and Vacuum Circuit Breaker Parameters on Transient Recovery Voltage. In Proceedings of the 2010 Asia-Pacific Power and Energy Engineering Conference, Chengdu, China, 28–31 March 2010; pp. 1–4. [\[CrossRef\]](#)
14. Popov, M.; Gustavsen, B.; Martinez-Velasco, J.A. Transformer modelling for impulse voltage distribution and terminal transient analysis. In *Electromagnetic Transients in Transformer and Rotating Machine Windings*; IGI Global: Hershey, PA, USA, 2013; pp. 239–320.
15. Glinkowski, M.; Piasecki, W.; Florkowski, M.; Fulczyk, M.; Arauzo, F. SmartChoke-protecting power equipment from fast transients. In Proceedings of the 2008 IEEE/PES Transmission and Distribution Conference and Exposition, Chicago, IL, USA, 21–24 April 2008.
16. CIGRE. Guidelines for representation of network elements when calculating transients. *CIGRE Tech. Broch.* **1990**, *30*.

17. International Electrotechnical Commission. *IEC 60071-1 Insulation Coordination—Part 1: Definitions, Principles and Rules*; International Electrotechnical Commission: Geneva, Switzerland, 1993.
18. Martinez-Velasco, J.A. Introduction to electromagnetic transient analysis of power systems. In *Transient Analysis of Power Systems: Solution Techniques, Tools and Applications*; Wiley: Hoboken, NJ, USA, 2015; pp. 1–8.
19. Bayless, R.; Selman, J.; Truax, D.; Reid, W. Capacitor switching and transformer transients. *IEEE Trans. Power Deliv.* **1988**, *3*, 349–357. [[CrossRef](#)]
20. Mombello, E.E.; Moller, K. New power transformer model for the calculation of electromagnetic resonant transient phenomena including frequency-dependent losses. *IEEE Trans. Power Deliv.* **2000**, *15*, 167–174. [[CrossRef](#)]
21. Van Craenenbroeck, T.; De Ceuster, J.; Marly, J.; De Herdt, H.; Brouwers, B.; Van Dommelen, D. Experimental and numerical analysis of fast transient phenomena in distribution transformers. In Proceedings of the 2000 IEEE Power Engineering Society Winter Meeting. Conference Proceedings (Cat. No. 00CH37077), Singapore, 23–27 January 2000.
22. De Herdt, H.; Declercq, J.; Sels, T.; Van Craenenbroeck, T.; Van Dommelen, D. Fast transients and their effect on transformer insulation: simulation and measurements. In Proceedings of the 16th International Conference and Exhibition on Electricity Distribution, 2001. Part 1: Contributions. CIRED. (IEE Conf. Publ. No. 482), Amsterdam, The Netherlands, 18–21 June 2001.
23. Diesendorf, W. *Insulation Co-Ordination in High-Voltage Electric Power Systems*; Newnes-Butterworth: Oxford, UK, 1974.
24. Mehinović, A.; Grebović, S.; Fežić, A.; Oprašić, N.; Konjicija, S.; Akšamović, A. Application of artificial intelligence methods for determination of transients in the power system. *Electr. Power Syst. Res.* **2023**, *223*, 109634. [[CrossRef](#)]
25. Arranz, R.; Paredes, Á.; Rodríguez, A.; Muñoz, F. Fault location in transmission system based on transient recovery voltage using Stockwell transform and artificial neural networks. *Electr. Power Syst. Res.* **2021**, *201*, 107569. [[CrossRef](#)]
26. IEEE. *Draft Guide for the Application of Neutral Grounding in Electrical Utility Systems, Part IV—Distribution*; IEEE: Piscataway, NJ, USA, 2014.
27. *Std C62.82.1-2010*; IEEE Standard for Insulation Coordination-Definitions, Principles, and Rules. IEEE: Piscataway, NJ, USA, 2011.
28. Othman, N.; Rohani, M.; Mustafa, W.; Wooi, C.; Rosmi, A.; Shakur, N.; Juliangga, R.; Khairunizam, W.; Zunaidi, I.; Razlan, Z.; et al. An Overview on Overvoltage Phenomena in Power Systems. In *IOP Conference Series: Materials Science and Engineering*; IOP Publishing: Bristol, UK, 2019; Volume 557, p. 012013.
29. Sima, W.; Zhang, H.; Yang, M.; Li, X. Diagnosis of small-sample measured electromagnetic transients in power system using DRN-LSTM and data augmentation. *Int. J. Electr. Power Energy Syst.* **2022**, *137*, 107820. [[CrossRef](#)]
30. Niazazari, I.; Jalilzadeh Hamidi, R.; Livani, H.; Arghandeh, R. Cause identification of electromagnetic transient events using spatiotemporal feature learning. *Int. J. Electr. Power Energy Syst.* **2020**, *123*, 106255. [[CrossRef](#)]
31. Hamzah, N.; Anuwar, F.H.; Zakaria, Z.; Tahir, N.M. Classification of transient in power system using support vector machine. In Proceedings of the 2009 5th International Colloquium on Signal Processing & Its Applications, Kuala Lumpur, Malaysia, 6–8 March 2009; pp. 418–422. [[CrossRef](#)]
32. Ekici, S. Classification of power system disturbances using support vector machines. *Expert Syst. Appl.* **2009**, *36*, 9859–9868. [[CrossRef](#)]
33. Asman, S.H.; Abidin, A.F.; Yusoh, M.A.T.M.; Subiyanto, S. Identification of transient overvoltage using discrete wavelet transform with minimised border distortion effect and support vector machine. *Results Eng.* **2022**, *13*, 100311. [[CrossRef](#)]
34. Thukaram, D.; Khincha, H.; Khandelwal, S. Estimation of switching transient peak overvoltages during transmission line energization using artificial neural network. *Electr. Power Syst. Res.* **2006**, *76*, 259–269. [[CrossRef](#)]
35. Erişti, H.; Uçar, A.; Demir, Y. Wavelet-based feature extraction and selection for classification of power system disturbances using support vector machines. *Electr. Power Syst. Res.* **2010**, *80*, 743–752. [[CrossRef](#)]
36. Velasco, J.M.; Mork, B. Transformer Modelling for Simulation of Low Frequency Transients in Power Systems. In Proceedings of the 17th International Conference on Electricity Distribution, Session, Barcelona, Spain, 12–15 May 2003; Volume 1.
37. Vakilian, M.; Degeneff, R.C. A method for modeling nonlinear core characteristics of transformers during transients. *IEEE Trans. Power Deliv.* **1994**, *9*, 1916–1925. [[CrossRef](#)]
38. Semlyen, A.; De Leon, F. Eddy current add-on for frequency dependent representation of winding losses in transformer models used in computing electromagnetic transients. *IEE Proc.-Gener. Transm. Distrib.* **1994**, *141*, 209–214. [[CrossRef](#)]
39. Martinez-Velasco, J.A. *Transient Analysis of Power Systems: A Practical Approach*; John Wiley & Sons: Hoboken, NJ, USA, 2020.
40. Velasco, J.A.M. *Power System Transients: Parameter Determination*; CRC Press: Boca Raton, FL, USA, 2010.
41. Rabins, L. A new approach to the analysis of impulse voltages and gradients in transformer windings. *Trans. Am. Inst. Electr. Eng. Part III Power Appar. Syst.* **1959**, *78*, 1784–1791. [[CrossRef](#)]
42. Guardado, J.; Cornick, K. A computer model for calculating steep-fronted surge distribution in machine windings. *IEEE Trans. Energy Convers.* **1989**, *4*, 95–101. [[CrossRef](#)] [[PubMed](#)]
43. Hoidalén, H.K.; Chiesa, N.; Avendaño, A.; Mork, B. *Developments in the Hybrid Transformer Model—Core Modeling and Optimization*; International Conference on Power Systems Transients (IPST 2011); IPST: Delft, The Netherlands, 2011.
44. Iravani, M.; Chaudhary, A.; Giesbrecht, W.; Hassan, I.; Keri, A.; Lee, K.; Martinez, J.; Morched, A.; Mork, B.; Parniani, M.; et al. Modeling and analysis guidelines for slow transients. III. The study of ferroresonance. *IEEE Trans. Power Deliv.* **2000**, *15*, 255–265. [[CrossRef](#)]
45. CIGRÉ. *Electrical Transient Interaction between Transformers and the Power System*; CIGRÉ: Paris, France, 2014.

46. Jazebi, S.; Zirka, S.; Lambert, M.; Rezaei-Zare, A.; Chiesa, N.; Moroz, Y.; Chen, X.; Martinez-Duro, M.; Arturi, C.; Dick, E.; et al. Duality derived transformer models for low-frequency electromagnetic transients—Part I: Topological models. *IEEE Trans. Power Deliv.* **2016**, *31*, 2410–2419. [[CrossRef](#)]
47. Álvarez-Mariño, C.; De León, F.; López-Fernández, X.M. Equivalent circuit for the leakage inductance of multiwinding transformers: Unification of terminal and duality models. *IEEE Trans. Power Deliv.* **2011**, *27*, 353–361. [[CrossRef](#)]
48. Jazebi, S.; De Leon, F.; Farazmand, A.; Deswal, D. Dual reversible transformer model for the calculation of low-frequency transients. *IEEE Trans. Power Deliv.* **2013**, *28*, 2509–2517. [[CrossRef](#)]
49. Tarasiewicz, E.; Morched, A.; Narang, A.; Dick, E. Frequency dependent eddy current models for nonlinear iron cores. *IEEE Trans. Power Syst.* **1993**, *8*, 588–597. [[CrossRef](#)]
50. De Leon, F.; Semlyen, A. Complete transformer model for electromagnetic transients. *IEEE Trans. Power Deliv.* **1994**, *9*, 231–239. [[CrossRef](#)]
51. Ljung, L. *System Identification—Theory for the User*, 2nd ed.; PTR Prentice-Hall: Upper Saddle River, NJ, USA, 1999.
52. Nelles, O. *Nonlinear System Identification*; Springer: Berlin/Heidelberg, Germany, 2002.
53. Ceceña, A.A. Transformer Modeling in ATP: Internal Faults & High-Frequency Discretization. Ph.D. Thesis, Michigan Technological University, Houghton, MI, USA, 2011.
54. Gustavsen, B. Wide band modeling of power transformers. *IEEE Trans. Power Deliv.* **2004**, *19*, 414–422. [[CrossRef](#)]
55. Gustavsen, B. Wideband transformer modeling including core nonlinear effects. *IEEE Trans. Power Deliv.* **2015**, *31*, 219–227. [[CrossRef](#)]
56. Morched, A.; Marti, L.; Ottevangers, J. A high frequency transformer model for the EMTP. *IEEE Trans. Power Deliv.* **1993**, *8*, 1615–1626. [[CrossRef](#)]
57. Gustavsen, B. A hybrid measurement approach for wideband characterization and modeling of power transformers. *IEEE Trans. Power Deliv.* **2010**, *25*, 1932–1939. [[CrossRef](#)]
58. Jazebi, S.; De León, F. Duality-based transformer model including eddy current effects in the windings. *IEEE Trans. Power Deliv.* **2015**, *30*, 2312–2320. [[CrossRef](#)]
59. Mork, B.A.; Gonzalez, F.; Ishchenko, D.; Stuehm, D.L.; Mitra, J. Hybrid transformer model for transient simulation—Part I: Development and parameters. *IEEE Trans. Power Deliv.* **2006**, *22*, 248–255. [[CrossRef](#)]
60. Rezaei-Zare, A. Enhanced transformer model for low-and mid-frequency transients—Part I: Model development. *IEEE Trans. Power Deliv.* **2014**, *30*, 307–315. [[CrossRef](#)]
61. Høidalen, H.K.; Rocha, A.C. Analysis of gray Box Modelling of Transformers. *Electr. Power Syst. Res.* **2021**, *197*, 107266. [[CrossRef](#)]
62. Kafshgari, N.A.; Ramezani, N.; Nouri, H. Effects of high frequency modeling & grounding system parameters on transient recovery voltage across vacuum circuit breakers for capacitor switching in wind power plants. *Int. J. Electr. Power Energy Syst.* **2019**, *104*, 159–168.
63. Degeneff, R. A general method for determining resonances in transformer windings. *IEEE Trans. Power Appar. Syst.* **1977**, *96*, 423–430. [[CrossRef](#)]
64. Fergestad, P.; Henriksen, T. Inductances for the calculation of transient oscillations in transformers. *IEEE Trans. Power Appar. Syst.* **1974**, *2*, 510–517. [[CrossRef](#)]
65. Keyhani, A.; Chua, S.; Sebo, S. Maximum likelihood estimation of transformer high frequency parameters from test data. *IEEE Trans. Power Deliv.* **1991**, *6*, 858–865. [[CrossRef](#)]
66. Degeneff, R.; McNutt, W.; Neugebauer, W.; Panek, J.; McCallum, M.; Honey, C. Transformer response to system switching voltages. *IEEE Trans. Power Appar. Syst.* **1982**, *101*, 1457–1470. [[CrossRef](#)]
67. Grover, F.W. *Inductance Calculations: Working Formulas and Tables*; Courier Corporation: North Chelmsford, MA, USA, 2004.
68. Kulkarni, S.V.; Khaparde, S. *Transformer Engineering*; Marcel Dekker: New York, NY, USA, 2004.
69. Venegas, V.; Guardado, J.; Melgoza, E.; Maximov, S.; Hernandez, M. A Computer Model for Transient Voltages Distribution Studies in Transformer Windings. In Proceedings of the 9th WSEAS/IASME International Conference, Florença, Italy, 23–25 August 2011; pp. 121–126.
70. Kulkarni, S.V.; Khaparde, S.A. *Transformer Engineering: Design, Technology, and Diagnostics*; CRC Press: Boca Raton, FL, USA, 2017.
71. Wirgau, K. Inductance calculation of an air-core disk winding. *IEEE Trans. Power Appar. Syst.* **1976**, *95*, 394–400. [[CrossRef](#)]
72. Rahimpour, E.; Bigdeli, M. Simplified transient model of transformer based on geometrical dimensions used in power network analysis and fault detection studies. In Proceedings of the 2009 International Conference on Power Engineering, Energy and Electrical Drives, Lisbon, Portugal, 18–20 March 2009.
73. Bellei, T.; Camm, E.; Ransom, G. Current-limiting inductors used in capacitor bank applications and their impact on fault current interruption. In Proceedings of the 2001 IEEE/PES Transmission and Distribution Conference and Exposition. Developing New Perspectives (Cat. No.01CH37294), Atlanta, GA, USA, 2 November, 2001; Volume 1, pp. 603–607. [[CrossRef](#)]
74. Liu, H.; Wang, Z.; Yang, J.; Li, B.; Ren, A. Circuit breaker Rate-of-Rise recovery voltage in Ultra-High voltage lines with hybrid reactive power compensation. *Energies* **2018**, *11*, 100. [[CrossRef](#)]
75. Martinez, J.; Durbak, D. Parameter determination for modeling systems transients-Part V: Surge arresters. *IEEE Trans. Power Deliv.* **2005**, *20*, 2073–2078. [[CrossRef](#)]

76. Sakshaug, E. Influence of rate-of-rise on distribution arrester protective characteristics. *IEEE Trans. Power Appar. Syst.* **1979**, *98*, 519–526. [[CrossRef](#)]
77. Tominaga, S.; Azumi, K.; Shibuya, Y.; Imataki, M.; Fujiwara, Y.; Nishida, S. Protective performance of metal oxide surge arrester based on the dynamic vi characteristics. *IEEE Trans. Power Appar. Syst.* **1979**, *98*, 1860–1871. [[CrossRef](#)]
78. Lat, M. Analytical method for performance prediction of metal oxide surge arresters. *IEEE Trans. Power Appar. Syst.* **1985**, *104*, 2664–2674. [[CrossRef](#)]
79. Durbak, D. The choice of EMTP surge arrester models. *EMTP Newsl.* **1987**, *7*, 14–18.
80. Schmidt, W.; Meppelink, J.; Richter, B.; Feser, K.; Kehl, L.; Qui, D. Behaviour of MO-surge-arrester blocks to fast transients. *IEEE Trans. Power Deliv.* **1989**, *4*, 292–300. [[CrossRef](#)]
81. Popov, M.; Van Der Sluis, L.; Paap, G. Investigation of the circuit breaker reignition overvoltages caused by no-load transformer switching surges. *Eur. Trans. Electr. Power* **2001**, *11*, 413–422. [[CrossRef](#)]
82. Jones, R.; Clifton, P.; Grotz, G.; Lat, M.; Lembo, F.; Melvold, D.; Nigol, D.; Skivtas, J.; Sweetana, A.; Goodwin, D.; et al. Modeling of metal-oxide surge arresters. *IEEE Trans. Power Deliv.* **1992**, *7*, 302–309.
83. Pinceti, P.; Giannettoni, M. A simplified model for zinc oxide surge arresters. *IEEE Trans. Power Deliv.* **1999**, *14*, 393–398. [[CrossRef](#)]
84. Dommel, H.W. Digital computer solution of electromagnetic transients in single-and multiphase networks. *IEEE Trans. Power Appar. Syst.* **1969**, *88*, 388–399. [[CrossRef](#)]
85. Keri, A.; Gole, A.; Martinez-Velasco, J. *Modeling and Analysis of System Transients Using Digital Programs*; IEEE Special Publication; IEEE: Piscataway, NJ, USA, 1998.
86. Marti, L. Simulation of transients in underground cables with frequency-dependent modal transformation matrices. *IEEE Trans. Power Deliv.* **1988**, *3*, 1099–1110. [[CrossRef](#)]
87. Nelms, R.; Sheble, G.; Newton, S.R.; Grigsby, L. Using a personal computer to teach power system transients. *IEEE Trans. Power Syst.* **1989**, *4*, 1293–1294. [[CrossRef](#)] [[PubMed](#)]
88. Macias, J.; Exposito, A.; Soler, A. A comparison of techniques for state-space transient analysis of transmission lines. *IEEE Trans. Power Deliv.* **2005**, *20*, 894–903. [[CrossRef](#)]
89. Dommel, H.W. *Electromagnetic Transients Program Reference Manual*; Bonneville Power Administration: Portland, OR, USA, 1986, p. 4.
90. Marti, J.R. Accurate modelling of frequency-dependent transmission lines in electromagnetic transient simulations. *IEEE Trans. Power Appar. Syst.* **1982**, *101*, 147–157. [[CrossRef](#)]
91. Zubiaga, M.; Aurtenetxea, S. *Energy Transmission and Grid Integration of AC Offshore Wind Farms*; IntechOpen: London, UK, 2012.
92. Kurokawa, S.; Costa, E.C.; Pissolato, J.; Prado, A.J.; Bovolato, L.F. Proposal of a transmission line model based on lumped elements: An analytic solution. *Electr. Power Compon. Syst.* **2010**, *38*, 1577–1594. [[CrossRef](#)]
93. Mangelrød, B.; Kent, D.B.K. Transmission line models for the simulation of interaction phenomena between parallel AC and DC overhead lines. In Proceedings of the International Conference on Power Systems Transients, Budapest, Hungary, 20 June–24 June 1999; pp. 20–24.
94. Morched, A.; Gustavsen, B.; Tartibi, M. A universal model for accurate calculation of electromagnetic transients on overhead lines and underground cables. *IEEE Trans. Power Deliv.* **1999**, *14*, 1032–1038. [[CrossRef](#)]
95. Noda, T.; Nagaoka, N.; Ametani, A. Phase domain modeling of frequency-dependent transmission lines by means of an ARMA model. *IEEE Trans. Power Deliv.* **1996**, *11*, 401–411. [[CrossRef](#)]
96. Niu, S.; Wang, W. Abnormal trip analysis of circuit breaker in 220 kV substation. In Proceedings of the 2019 IEEE 3rd Information Technology, Networking, Electronic and Automation Control Conference (ITNEC), Chengdu, China, 15–17 March, 2019; pp. 210–213. [[CrossRef](#)]
97. Swanson, B.W.; Roidt, R.M. Boundary Layer Analysis of an SF6 Circuit Breaker Arc. *IEEE Trans. Power Appar. Syst.* **1971**, *90*, 1086–1093. [[CrossRef](#)]
98. Martinez, J.; Mahseredjian, J.; Khodabakhchian, B. Parameter determination for modeling system transients-Part VI: Circuit breakers. *IEEE Trans. Power Deliv.* **2005**, *20*, 2079–2085. [[CrossRef](#)]
99. CIGRE. *Guidelines for Representation of Networks: Elements when Calculating Transients*; CIGRE: Paris, France, 1994.
100. Rifaat, R.; Lally, T.S.; Hong, J. Circuit breaker transient recovery voltage requirements for medium voltage systems with NRG. In Proceedings of the 2013 IEEE Industry Applications Society Annual Meeting, Lake Buena Vista, FL, USA, 6–11 October, 2013; pp. 1–6. [[CrossRef](#)]
101. Faried, S.; Elsamahy, M. Incorporating superconducting fault current limiters in the probabilistic evaluation of transient recovery voltage. *IET Gener. Transm. Distrib.* **2011**, *5*, 101–107. [[CrossRef](#)]
102. Bagherpoor, A.; Rahimi-Pordanjani, S.; Razi-Kazemi, A.A.; Niayesh, K. Online Condition Assessment of Interruption Chamber of Gas Circuit Breakers Using Arc Voltage Measurement. *IEEE Trans. Power Deliv.* **2017**, *32*, 1776–1783. [[CrossRef](#)]
103. Mayr, O. Beiträge zur Theorie des statischen und des dynamischen Lichtbogens. *Arch. Elektrotech.* **1943**, *37*, 588–608. [[CrossRef](#)]
104. Cassie, A.M. *Arc Rupture and Circuit Severity: A New Theory*; CIGRE Report; CIGRE: Paris, France, 1939.
105. Ala, G.; Inzerillo, M. An Improved Circuit-Breaker Model in MODELS Language. In Proceedings of the International Conference on Power System Transients, Budapest, Hungary, 1999.

106. Nitu, S.; Nitu, C.; Anghelita, P. Electric Arc Model, for High Power Interrupters. In Proceedings of the EUROCON 2005-The International Conference on “Computer as a Tool”, Belgrade, Serbia, 21–24 November 2005.
107. Dufournet, D. *Transient Recovery Voltages for High-Voltage Circuit Breakers—Part 1*; Tech. Rep.; Alstom Grid: San Antonio, TX, USA, 2013; pp. 1–186.
108. Palazzo, M.; Popov, M.; Marmolejo, A.; Delfanti, M. Revision of TRV requirements for the application of generator circuit-breakers. *Electr. Power Syst. Res.* **2016**, *138*, 66–71. [[CrossRef](#)]
109. Park, R.H.; Skeats, W.F. Circuit Breaker Recovery Voltages Magnitudes and Rates of Rise. *Trans. Am. Inst. Electr. Eng.* **1931**, *50*, 204–238. [[CrossRef](#)]
110. Boehne, E.W. The determination of circuit recovery rates. *Electr. Eng.* **1935**, *54*, 530–539. [[CrossRef](#)]
111. Adams, J.A.; Skeats, W.F.; Van Sickle, R.C.; Sillers, T.G.A. Practical calculation of circuit transient recovery voltages. *Electr. Eng.* **1942**, *61*, 771–779. [[CrossRef](#)]
112. Clair, H.P.S.; Adams, J.A. Transient recovery-voltage characteristics of electric-power systems. *Electr. Eng.* **1942**, *61*, 666–668. [[CrossRef](#)]
113. Browne, T.E. Practical Modeling of the Circuit Breaker ARC as a Short Line Fault Interrupter. *IEEE Trans. Power Appar. Syst.* **1978**, *97*, 838–847. [[CrossRef](#)]
114. Slepian, J. Extinction of an A-C. Arc. *Trans. Am. Inst. Electr. Eng.* **1928**, *47*, 1398–1407. [[CrossRef](#)]
115. Colclaser, R.G.; Buettner, D.E. The Traveling-Wave Approach to Transient Recovery Voltage. *IEEE Trans. Power Appar. Syst.* **1969**, *88*, 1028–1035. [[CrossRef](#)]
116. Junxiang, L.; Guopei, W.; Wenxiong, M.; Kaijian, W.; Zhao, Y.; Yong, W.; Huihong, H. Impact of high coupled split reactor on the RRRV in the interrupting process of paralleled circuit breakers. In Proceedings of the 2018 IEEE Power & Energy Society General Meeting (PESGM), Portland, Oregon, USA, 5–10 August 2018.
117. Janhunen, O.P.; Nepola, K.; Rauhala, T. *Assessment of Measures to Improve Cost-Effective-Ness, Reliability and TRV Risk Management in Finnish Series Compensated System*; IPST: College Park, MD, USA, 2019.
118. Marini, P. *Impact of De-Energization of 33 kV Harmonic Filter on TRV of Vacuum Circuit Breaker*; IPST: College Park, MD, USA, 2019.
119. Koch, D. SF6 properties, and use in MV and HV switchgear. *Cah. Tech.* **2003**, *188*, 4.
120. Zhou, S.; Teng, F.; Tong, Q. Mitigating sulfur hexafluoride (SF6) emission from electrical equipment in China. *Sustainability* **2018**, *10*, 2402. [[CrossRef](#)]
121. Das, J.C.; Mohla, D.C. Harmonization of ANSI/IEEE standards for high-voltage circuit breakers with IEC and its impact on application and analysis. In Proceedings of the IEEE/IAS Pulp & Paper Industry Technical Paper Conference, Nashville, TN, USA, 19–23 June 2011.
122. Pramana, P.A.A.; Kusuma, A.A.; Harsono, B.B.S.; Munir, B.S. Simulation Study of Circuit Breaker Failure on Extra High Voltage Reactor. In Proceedings of the 2019 1st International Conference on Cybernetics and Intelligent System (ICORIS), Denpasar, Indonesia, 22–23 August 2019.
123. Wagner, C.L.; Dufournet, D.; Montillet, G.F. Revision of the application guide for transient recovery voltage for AC high-voltage circuit breakers of IEEE C37. 011: A working group paper of the high voltage circuit breaker subcommittee. *IEEE Trans. Power Deliv.* **2006**, *22*, 161–166. [[CrossRef](#)]
124. Chandankar, S.S.; Bhole, A.A. To Investigate Impacts of Various Factors on the Characteristics of Transient Recovery Voltage. *Int. J. Adv. Res. Electr. Instrum. Eng.* **2016**, *5*, 8821–8825.
125. Saied, M.M. The kilometric faults: Modeling and normalized relations for line transients and the breaker-recovery voltage. *IEEE Trans. Power Deliv.* **2005**, *20*, 1025–1030. [[CrossRef](#)]
126. Todeschini, G. Analysis of the effect of distance on the TRV waveform for a short-line fault. In Proceedings of the PES T&D 2012, Orlando, FL, USA, 7–10 May 2012.
127. Skeats, W.F.; Titus, C.H.; Wilson, W.R. Severe Rates of Rise of Recovery Voltage Associated with Transmission Line Short Circuits. *Trans. Am. Inst. Electr. Eng. Part III Power Appar. Syst.* **1957**, *76*, 1256–1264. [[CrossRef](#)]
128. Hedman, D.; Lambert, S. Power circuit breaker transient recovery voltages. *IEEE Trans. Power Appar. Syst.* **1976**, *95*, 197–207. [[CrossRef](#)]
129. Filipovic-Grcic, B.; Stipetic, N.; Vukovic, F.; Jerkovic, A.; Sanic, M.; Musulin, K. Transient recovery voltage investigation on HV circuit breaker in hydro power plant. *Electr. Power Syst. Res.* **2023**, *220*, 109306. [[CrossRef](#)]
130. Das, J. TRV (transient recovery voltage) in high voltage current interruption. *IEEE Trans. Ind. Appl.* **2018**, *55*, 2165–2172. [[CrossRef](#)]
131. *Std C37.011-1994*; IEEE Application Guide for Transient Recovery Voltage for AC High-Voltage Circuit Breakers Rated on a Symmetrical Current Basis. IEEE: Piscataway, NJ, USA, 1995; pp. 1–48. [[CrossRef](#)]
132. *IEEE Std C37.06-2009*; IEEE Standard for AC High-Voltage Circuit Breakers Rated on a Symmetrical Current Basis—Preferred Ratings and Related Required Capabilities for Voltages Above 1000 V. IEEE: Piscataway, NJ, USA, 2009; pp. 1–56. [[CrossRef](#)]
133. International Electrotechnical Commission. *High-Voltage Switchgear and Controlgear—Part 100: High-Voltage Alternating-Current Circuit Breakers*; International Electrotechnical Commission (IEC): Geneva, Switzerland, 2001; p. 62271-100.
134. Arranz, R.; Rodríguez, A.; Muñoz, F. Detection of the natural frequency of transmission power lines applying S-transform on Transient Recovery Voltage. *Electr. Power Syst. Res.* **2020**, *182*, 106142. [[CrossRef](#)]

135. Sălceanu, C.E.; Nicola, M.; Nicola, C.I.; Ocoleanu, D.; Dobrea, C.; Iovan, D.; Enache, S. Experimental Study on the Behavior of Aluminum Fuse Element Inside 24 kV, 50 kA High-Voltage Fuses. *Energies* **2022**, *15*, 7171. [[CrossRef](#)]
136. Swindler, D.; Schwartz, P.; Hamer, P.; Lambert, S. Transient recovery voltage considerations in the application of medium-voltage circuit breakers. *IEEE Trans. Ind. Appl.* **1997**, *33*, 383–388. [[CrossRef](#)]
137. Awad, E.; Badran, E.A. Mitigation of Transient Recovery Voltages using the Supercapacitor. *MEJ Mansoura Eng. J.* **2020**, *45*, 37–42. [[CrossRef](#)]
138. *IEEE Std C37.04-2018 (Revision of IEEE Std C37.04-1999)*; IEEE Standard for Ratings and Requirements for AC High-Voltage Circuit Breakers with Rated Maximum Voltage Above 1000 V. IEEE: Piscataway, NJ, USA, 2019; pp. 1–122. [[CrossRef](#)]
139. Watson, N.; Arrillaga, J.; Arrillaga, J. *Power Systems Electromagnetic Transients Simulation*; IET: Stevenage, UK, 2003; Volume 39.
140. Dommel, H.W. Nonlinear and time-varying elements in digital simulation of electromagnetic transients. *IEEE Trans. Power Appar. Syst.* **1971**, *90*, 2561–2567. [[CrossRef](#)]
141. Dommel, H.W.; Meyer, W.S. Computation of electromagnetic transients. *Proc. IEEE* **1974**, *62*, 983–993. [[CrossRef](#)]
142. Das, J. *Transients in Electrical Systems: Analysis, Recognition, and Mitigation*; McGraw-Hill Professional Publishing: New York, NY, USA, 2010.
143. Wagner, C.L.; Smith, H.M. Analysis Of Transient Recovery Voltage (TRV) Rating Concepts. *IEEE Trans. Power Appar. Syst.* **1984**, *103*, 3353–3363. [[CrossRef](#)]
144. Kocar, I.; Mahseredjian, J. Accurate frequency dependent cable model for electromagnetic transients. *IEEE Trans. Power Deliv.* **2015**, *31*, 1281–1288. [[CrossRef](#)]
145. Franco, M.; Caetano, M.; Bonatto, B.; Passaro, M. Modeling and normative instructions for the application of EMT-based programs in the evaluation of medium voltage circuit-breakers in a real industrial system. *Electr. Power Syst. Res.* **2023**, *223*, 109627. [[CrossRef](#)]
146. Yang, J.; Liu, H.; Sun, Y.; Li, Q.; Han, M.; Duan, Y.; Wang, X. Influence of UHV hybrid reactive power compensation on interrupting characteristics of circuit breakers in the event of phase-to-phase faults. *Int. J. Electr. Power Energy Syst.* **2021**, *124*, 106354. [[CrossRef](#)]

Disclaimer/Publisher’s Note: The statements, opinions and data contained in all publications are solely those of the individual author(s) and contributor(s) and not of MDPI and/or the editor(s). MDPI and/or the editor(s) disclaim responsibility for any injury to people or property resulting from any ideas, methods, instructions or products referred to in the content.